NASA/USRA HIGH ALTITUDE RESEARCH AIRCRAFT

GRYPHON

SOAR LIKE AN EAGLE WITH THE ROAR OF A LION

SPRING QUARTER, 1991

(NASA-CR-190002) NASA/USRA HIGH ALTITUDE RESEARCH AIRCRAFT. GRYPHON: SOAR LIKE AN EAGLE WITH THE ROAR OF A LION Final Report (USRA) 104 p

N92-21448

CSCL 01C

Unclas

G3/05 0073918

TEAM MEMBERS

JOSE RIVERA - PROJECT CO-MANAGER
PERFORMANCE

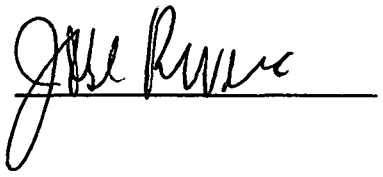

ANNE NUNES - PROJECT CO-MANAGER
PROPULSION

MIKE McRAY - AERODYNAMICS
ENGINE COOLING

WALTER WONG - STABILITY/CONTROL
FLYING QUALITIES

AUDREY ONG - HUMAN FACTORS
COST/AVIONICS

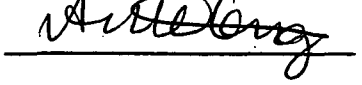

SCOTT COBLE - STRUCTURES
GRAPHICS

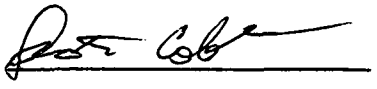

TABLE OF CONTENTS

LIST OF FIGURES

LIST OF TABLES

LIST OF SYMBOLS

A - Aspect ratio

a - Airfoil/aircraft interaction parameter

a.c. - Aerodynamic center

b - Wing span

Cd - Coefficient of drag

Cl - Coefficient of lift

Cm - Pitching moment coefficient

c.g. - Center of gravity

CT - Thrust coefficient

e - Oswald's efficiency factor

f - Equivalent parasitic drag area

fs - Fuel specific energy

GN2 - Ground nitrogen

h - Temperature difference

M - Mach number

n - Load factor

o.p. - Operating point

Ps - Specific energy

q - Dynamic pressure

r = $(Cd\ @\ Cl_{op} - Cd_{min})/(Cl_{op}^2)$

S - Planform area

TOGW - Takeoff gross weight

V - Velocity

α - Angle of attack

β - Sideslip angle

ABSTRACT

At the equator, the ozone layer ranges from 65,000 to 130,000+ feet which is beyond the capabilities of the ER-2, NASA's current high altitude reconnaissance aircraft. The Universities Space Research Association, in cooperation with NASA, is sponsoring an undergraduate program which is geared to designing an aircraft that can study the ozone layer at the equator. This aircraft must be able to satisfy four mission profiles. Mission one is a polar mission which ranges from Chile to the South Pole and back to Chile, a total range of 6000 n. mi at 100,000 feet with a 2500 lb. payload. The second mission is also a polar mission with a decreased altitude of 70,000 feet and an increased payload of 4000 lb. For the third mission, the aircraft will take-off at NASA Ames, cruise at 100,000 feet carrying a 2500 lb. payload, and land in Puerto Montt, Chile. The final mission requires the aircraft to take-off at NASA Ames, cruise at 100,000 feet with a 1000 lb. payload, make an excursion to 120,000 feet, and land at Howard AFB, Panama. All three missions require that a subsonic Mach number be maintained due to constraints imposed by the air sampling equipment. The aircraft need not be manned for all four missions. Three aircraft configurations have been determined to be the most suitable for meeting the above requirements. The performance of each configuration is analyzed to investigate the feasibility of

the project requirements. In the event that a requirement can not be obtained within the given constraints, recommendations for proposal modifications are given.

INTRODUCTION

The reasons for creating a high altitude aircraft have already been explained in the abstract of this report. This volume of the proposal deals with a tandem - wing twin - fuselage configuration called the "GRYPHON". The airplane has been designed to meet most of the requirements that were specified in the RFP sent out by NASA. Included in this report are discussions of the research involved in finding the best components for the airplane, detailed descriptions of the specifications of these components, an addressing of the design drivers for the project, and suggestions for the solution of any remaining problems. The report was not written to discuss every possibility for the airplane, but rather, to explain the Gryphon's configuration and capabilities.

Ozone Problem

An understanding of the variability of global ozone has become increasingly important because of its relevance to life on Earth. Since the ozone overburden controls the amount of incident near-ultraviolet solar radiation reaching the Earth's surface, sampling of the stratosphere up to 100,000 ft is needed so that accurate, detailed chemical and particle analysis can be performed.

Natural chemical reactions break down the ozone molecule but this is not as alarming as the rate of major ozone

modifying substances released by human activities. Though some chemicals released by mankind's activities, particularly carbon dioxide and methane, increase ozone, the more chlorofluorocarbon emissions increase, the faster ozone depletion is expected to occur.

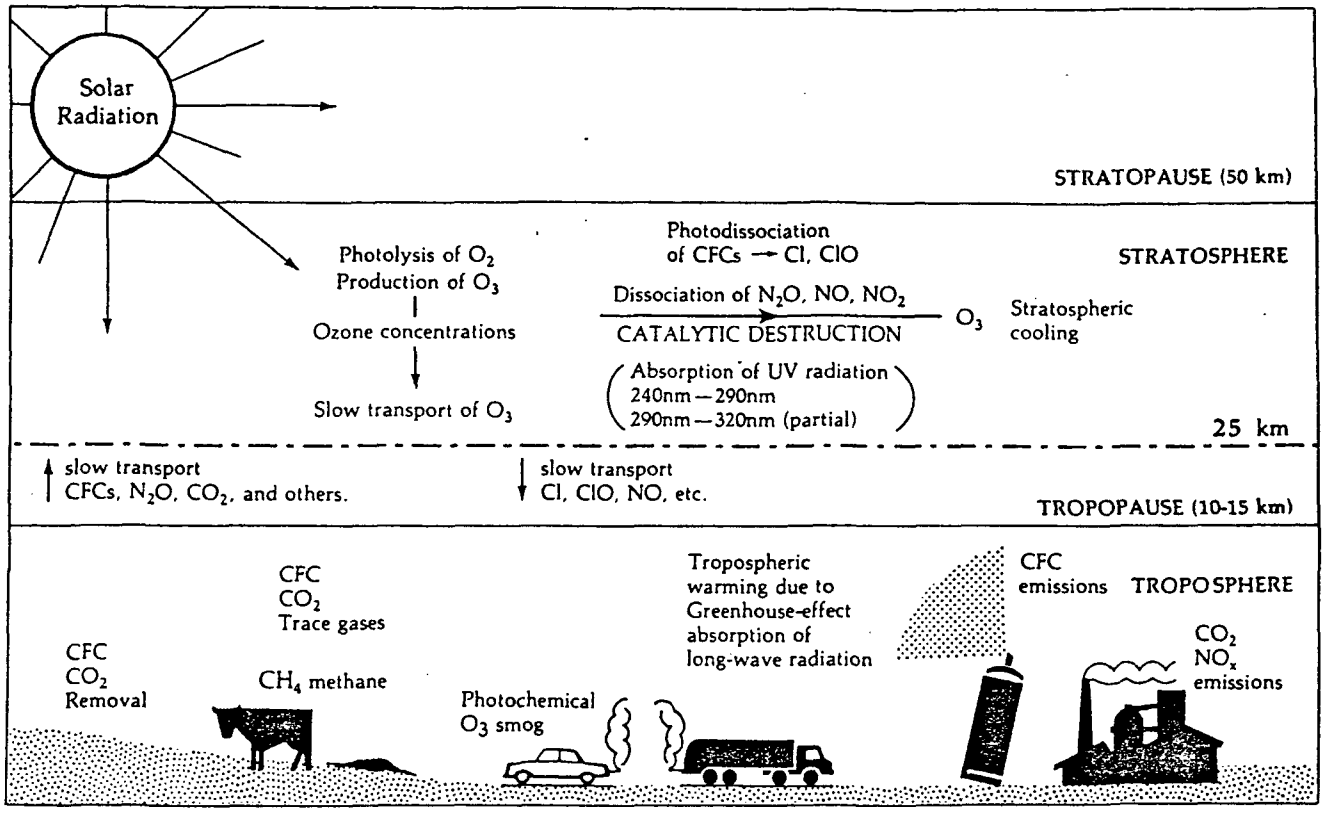

Figure 1: Destruction of Ozone by Chemical Processes

Chlorofluorocarbons and other chemicals are not broken down in the troposphere, instead, they are carried up to the ozone layer by the atmosphere's normal turbulent mixing and, after six to eight years, reach the stratosphere. Once there, the chemicals can survive for up to 100 years. When they are broken down, each chlorine atom can react with ozone and is

capable of destroying tens of thousands of ozone molecules before it eventually gets washed out of the atmosphere.

Gases now riding through the lower atmosphere will take up to eight years to reach the stratosphere. And, an additional 2 million tons of substances containing chlorine and bromine are still on the ground, trapped in insulation foams, appliances, and fire-fighting equipment. The high altitude missions are necessary to sample the ozone layer, find those areas that have been destroyed (holes above the South Pole), and check on the continual destruction of the atmosphere.

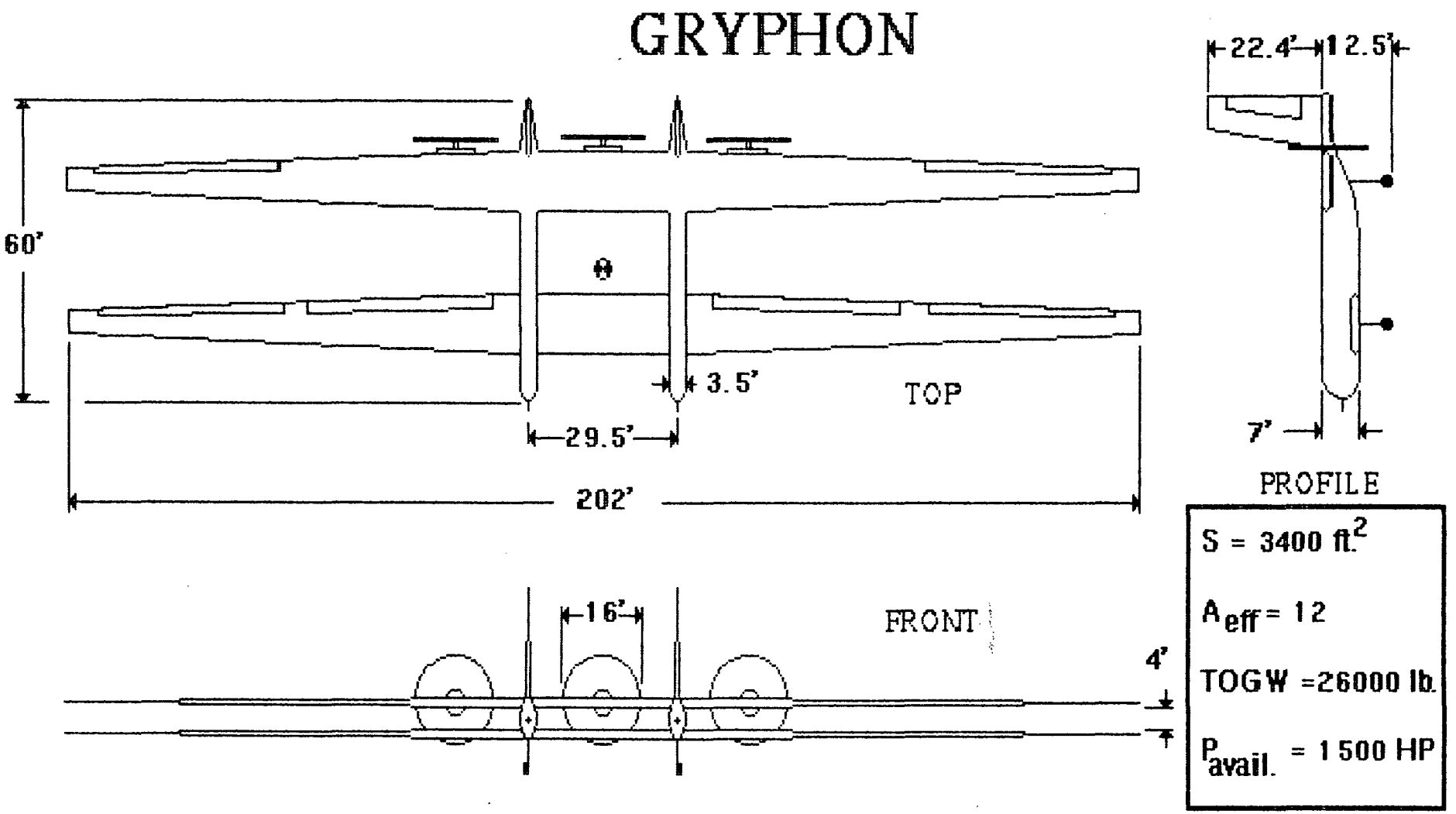
GRYPHON
60'
3.5'
TOP
29.5'
202'
16'
FRONT
4'
22.4'
12.5'
7'
PROFILE
S = 3400 ft.2
Aeff = 12
TOGW =26000 lb.
Pavail. = 1500 HP

Figure 2

CONFIGURATION SELECTION

The objective of this proposal is to design a high-altitude long-endurance aircraft that can carry payloads of up to 4,000 pounds and cruise within the subsonic regime. Because of the relatively low densities at high altitudes, the need for producing the necessary lift and thrust during flight drove the design. To address these problems, several factors were considered in selecting the best configuration:

- -lightweight aircraft that can support large lift loads
- -minimize induced drag associated with high-lift
- -high L/D
- -maintain flow over wing at low Reynolds numbers
- -accommodations for a large propulsion system

Four general configurations were considered for the design. The joined-wing configuration was investigated for its structural advantages over conventional configurations. However, it was discarded due to stability and control problems, and was relatively unproven. The biplane was investigated for its structural advantages and for the promise of a smaller wing span compared to conventional configurations. This idea was rejected due to the high drag it produced at high subsonic speeds. The conventional configuration was investigated for its simplicity and the massive data base available for analysis. However, to meet

the cruise requirements, the lifting surfaces would have to be very large, which would present structural problems.

The configuration that was selected for the high-altitude design was the Gryphon [Figure 2]. The tandem-wing configuration was selected for its lower induced drag. Theoretically, by distributing the weight of the aircraft into two lifting surfaces, the resulting induced drag is half that of a mono-wing with similar geometric characteristics (CDi is a function of CL^2). However, due to the interference effects between the two wings, the 50% reduction in induced drag is not fully realized. A negative stagger was used to place the rear wing away from the downwash of the front, which decreases the interference effects.

The twin-fuselage configuration was chosen to alleviate the bending moments on the wings and to increase its structural rigidity. This also provides more volume for payload. When the aircraft is to be manned, the cockpit will be located in the front of one of the fuselages, while the payload will be in the other fuselage. The sensors carried in the payload will have multi-directional access, so the data collection will not be restricted. Because large propellers were necessary for the Gryphon, the pusher configuration was chosen to decrease the propwash effects. A special feature worth noting is the elongated fuselage cross-section. This provides more gap between the negatively staggered tandem-

wings which results in less interference effects. Also, since the engines are mounted on the rear high-wing, it provides more ground clearance for the props.

The Gryphon does not have a horizontal tail. Power requirements at cruise made it necessary to mount a third engine between the vertical tails. Trim and pitch control is accomplished by the front wing, which is fitted with ailerons and flaps.

There are inherent problems associated with the Gryphon's configuration. Locating the three engines on the rear wing results in longitudinal stability problems. The use of stability augmentation systems, and effective distribution of payload and fuel might alleviate this problem.

Twin fuselages increase the rolling moment of inertia of the aircraft and make roll control more difficult. Larger control surfaces will have to be used. The controllability of the Gryphon is discussed in another section.

Another aspect of the Gryphon that needs to be investigated more fully is the aeroelastic effect due to the tandem-wing twin fuselage combination. The center section of the Gryphon might be subjected to disrupted flow due to the discontinuities in the configuration. These problems were beyond the scope of our design.

WEIGHT BREAKDOWN

The high altitude missions for which the Gryphon was designed have several design drivers. One of the most important ones was the requirement of low structural weight. The weight of the aircraft was a major factor in the structural design, the propulsion system determination, and many other fields. Using composites, it was possible to reduce the weight of the Gryphon, until the largest contributor to the gross take-off weight of the airplane was the fuel and engine weight. Figure 3 shows the weight breakdown for Missions one and four. The weights for the first three missions were similar, so only one breakdown is shown for these missions. The only variable weights in the plane were the fuel and payload weights. This was due to the fact that each mission has different altitude and payload requirements, as prescribed in the RFP. The take-off gross weight for Missions one through three are within 900 pounds of each other. Mission four has a TOGW of only 19670 pounds because it is a shorter mission with a very small payload.

GRYPHON WEIGHT PROFILE

MISSION 1

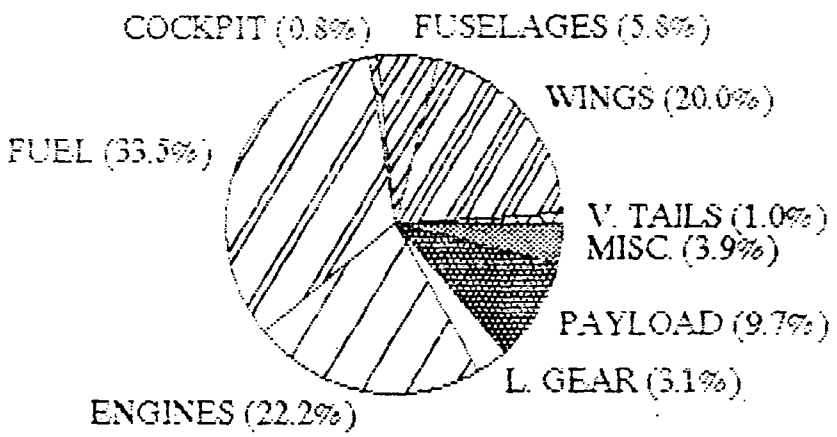

GROSS TAKE-OFF WEIGHT = 25670 POUNDS

(a)

GRYPHON WEIGHT PROFILE

MISSION 4

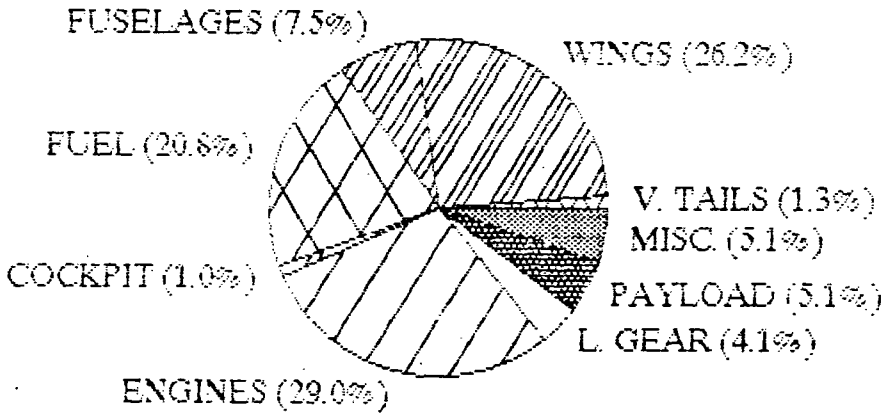

GROSS TAKE-OFF WEIGHT = 19670 POUNDS

(b)

Figure 3: Gryphon Weight Breakdown

AERODYNAMICS

The USRA/NASA High Altitude project requirements define the need for a vehicle that can climb to and sustain altitudes greater than 100,000 feet while remaining in subsonic flight. The implications of the mission requirements on the design and final configuration of the Gryphon are more pronounced and confining than in traditional aircraft.

The subject of utmost importance at high altitudes is low Reynolds number airflow and how it affects the airfoil design/integration process. Atmospheric conditions at 100,000 feet and a flight Mach number of .6 force the Reynolds number into the half million regime. At this Reynolds number the laminar separation bubble controls the separation characteristics of the airfoil. As it can be seen in Figure 4, this is detrimental to the airfoil's lift coefficient.

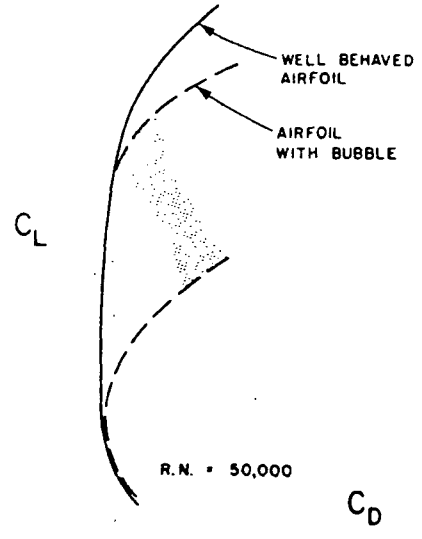

Figure 4: Effect of Laminar Bubble on Lift-Drag Polar

Vortex Generators

Submerged vortex generators have proven their ability to elongate laminar flow over the leading edge of the airfoil at low Reynolds numbers. This is accomplished by producing an eddy structure which gently induces a turbulent boundary layer further downstream. This eddy structure delays the onset of the laminar separation bubble and sets up a thinner turbulent boundary layer. The vortex generator has been tested in the wind tunnel and optimal results show a drag reduction of 38% without significantly altering the lifting characteristics of the airfoil. In the design of the Gryphon's wing, vortex generators will take the form of parabolic retractable ramps protruding from the leading edge of the airfoil to 40% chord. For the aft-loaded airfoil chosen for the tandem wing configuration, these vortex generators are necessary because the pitching moments are on the order of -0.17/radian. The vortex generators act in conjunction with a connecting tripwire as a transition tripping device. This serves to boost the drag polar of the airfoil to delay the onset of separation. The drag reductions caused by the use of vortex generators compensate for the unseen losses in trim drag that accompany any airfoil with a large pitching moment.

Airfoils

Several criteria drove the selection of the airfoil used for the High Flyer, including: $(Cl/Cd)_{max}$, low pitching moment, fore or aft loading, low Reynolds number profile, and airfoil thickness. The high lift to drag ratio (2-Dimensional) was required because of propulsion considerations. Basing the suitability of an airfoil on section properties, however, makes little sense, as such quantities do not account for the relationship between the airfoil and aircraft performance characteristics. For this airfoil design, figures of merit were used to address the suitability of the airfoil for the particular missions and characteristics of the vehicle. The figure of merit which leads to the maximum endurance for an aircraft is:

$$FOM = \{[e/(ea+1)]^3\}*[(Cl_{max}*b^2)/(f*Cl_{max}+k*Cd_{min})]$$

For a propeller-driven aircraft in which only b, W, e, V(min), and f are fixed, the airfoil which maximizes the figure of merit maximizes the aircraft endurance. This relationship is derived directly from the Breguet endurance formula. Figure 5 shows the drag polar of two different airfoils, the LA203A and the LNV109. Using these drag polars it is possible to construct a plot of the figure of merit vs. Cl_{max}. (Shown in Figure 6.) It was in this way that an airfoil was selected for the High Flyer.

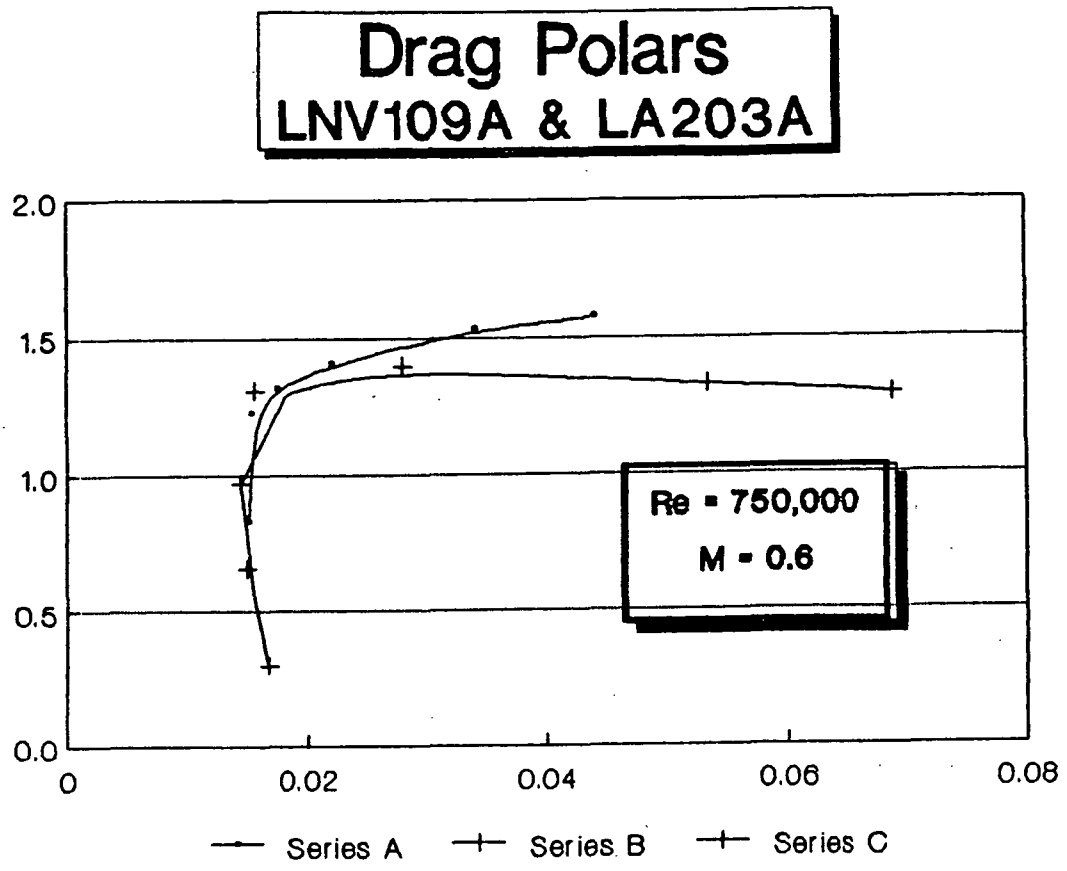

Figure 5

Maximum Endurance of airfoil; a tradeoff study

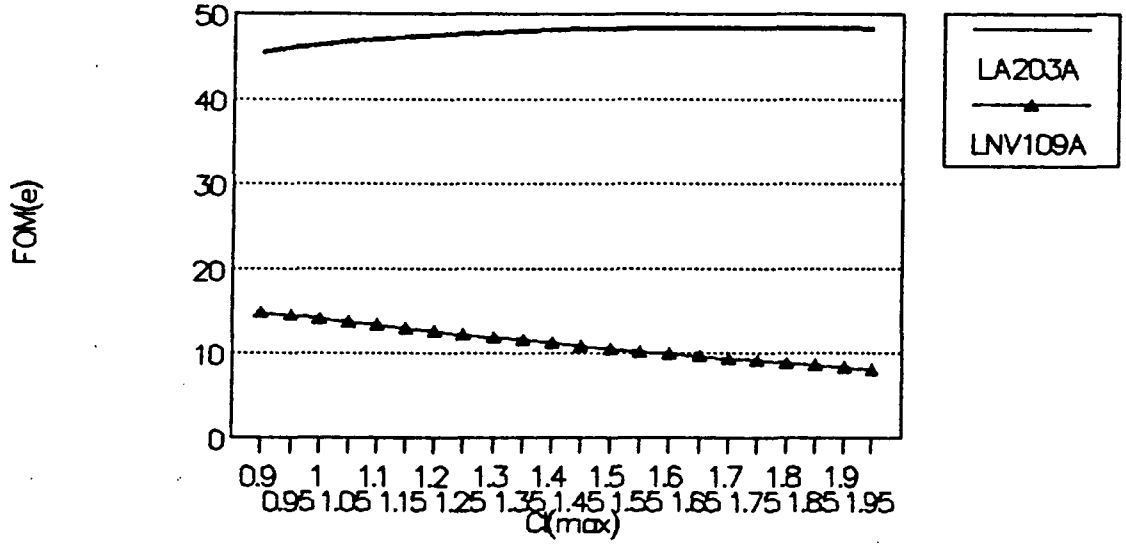

Figure 6

The brake horsepower of the engines is significantly reduced at high altitudes. This drives the need for low drag by reducing the available thrust to approximately 1000 lbs at 100,000 feet. The plane must be able to climb still further without increasing the flight velocity. This facilitates the need for a high lift coefficient to boost the ever dwindling rate of climb, thus driving the requirement for a high $(Cl/Cd)_{max}$.

The reasons for choosing a fore or aft loaded airfoil are anything but clearcut. Fore-loaded airfoils deliver higher design lift coefficients (> 1.3) without high pitching moment coefficients. The aft-loaded airfoils can attain maximum lift coefficients exceeding 1.65 with drag coefficients significantly less than the fore-loaded airfoils. Since trim drag can be decreased by means other than a low pitching moment coefficient, the aft-loaded airfoil was chosen due to its excellent lift to drag ratios. When one considers trim drag and total drag, these can be reduced to a minimum value in the Cm_0 range of -.15 to -.22. In accordance with the relationship:

$$Cm_0 = -.75\ Cl_{max}^2 + 2.365*Cl_{max} - 2.013$$

(Valid for Cl_{max} between 1.6 & 1.9)

Many airfoils were considered to satisfy these basic design criteria including: Eppler 660's, Lissaman 7769, Natural Laminar Flow Airfoils (NLF), the TH 25816, NACA 64-,

65-, and 66-series airfoils, Supercritical airfoils, Low Reynolds transonic (LRT) airfoils, and Liebeck airfoils. Each of these groups of airfoils, or a representative from the group was analyzed separately using the program X-Foil. The list of advantages and disadvantages of each of these airfoils is too extensive to go into at this point. The results of this airfoil pressure distribution and drag polar analysis pointed to a Liebeck airfoil called the LA203A, modified slightly by the subroutine GDES in XFOIL. The Liebeck LA203A airfoil exhibits the highest lift to drag ratio attainable at the Mach .6, Re = 500,000 design point, with total airplane lift/drag = 26. Other airfoils including the NLF 415 had higher Cl/Cd ratios at Re > 1 million but could not converge at lower Reynolds numbers using X-Foil.

The non-linearity of the change in an airfoil's drag polar with Reynolds number can be seen in Figure 7, which exhibits the LA203A at sea level Reynolds numbers and at high altitude Reynolds numbers. Notice that the drag polars yield increasingly higher drag penalties for the same lift coefficient as the Reynolds number increases. It is worthwhile to note that X-Foil uses a panel-vortex iteration procedure to produce pressure and velocity distributions over the airfoil section and to compute Cl, Cd, and Cm. Computational Fluid Dynamics (CFD) models are considered to be more reliable than panel methods in describing low Reynolds

number airflows. Marc Drella, the aerodynamicist who wrote the computer code XFOIL used it to design the Daedulus airfoil which flies at extremely low Reynolds numbers.

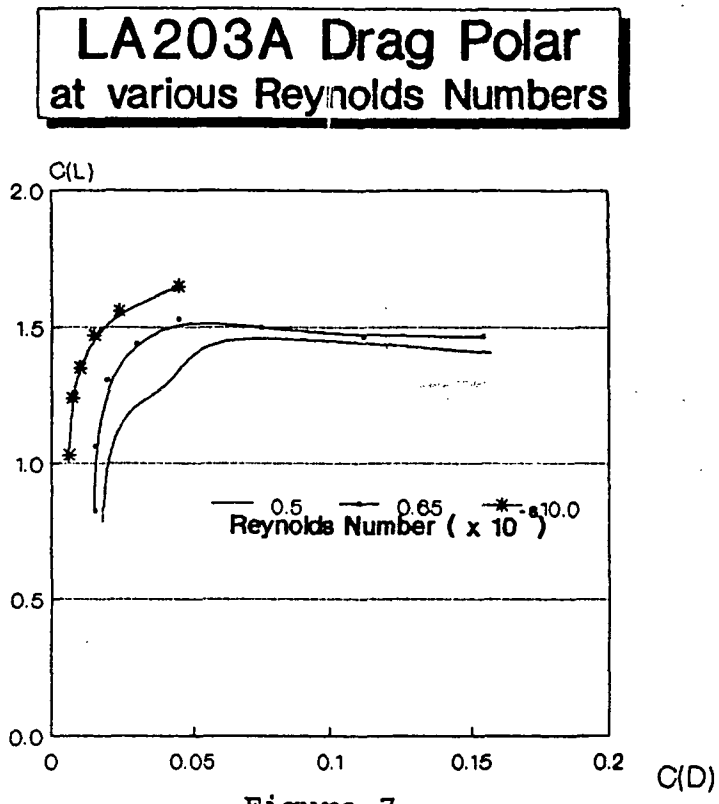

Figure 7

Aerodynamic Configuration Concerns

Tandem Wing - Twin Fuselage

The tandem wing configuration was chosen due to the theoretical 50% reduction in induced drag seen by displacing the aircraft weight over two lifting surfaces. This theoretical drag savings is somewhat less than 50% in practice due to the interference between the two wings. The twin fuselage configuration results in a penalty of twice the

wing/fuselage interference drag of a single fuselage, but it reduces the structural weight significantly.

The interference between the two wings in a tandem wing configuration can be greatly reduced by increasing the horizontal and vertical displacement between the two wings. The optimal spacing between the two wings involves tradeoffs between four parameters: lift coefficient, drag coefficient, lift/drag ratio, and moment coefficient. The results of the tradeoff studies (Figure 8) indicate that the vertical offset between the two wings should be -0.2, which correlates to a 2 foot vertical space between the Gryphon's wings. Optimal horizontal spacing is 2 chord lengths from the upstream airfoil's trailing edge to the downstream airfoil's leading edge which translates into a 16 foot space between the two wings (See Configuration).

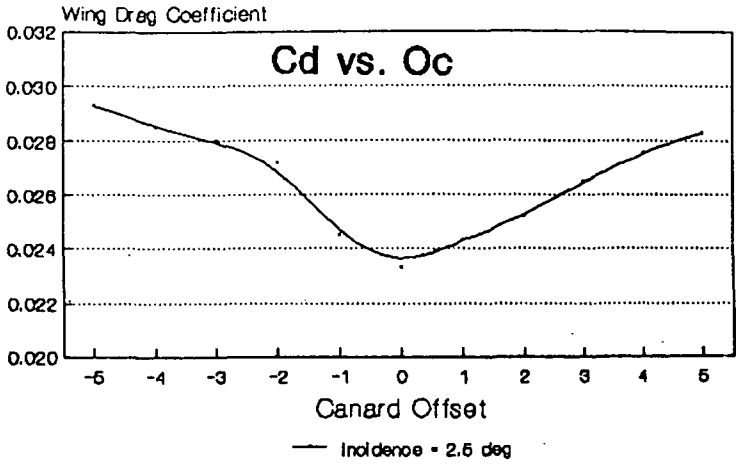
Wing Drag Coefficient
Cd vs. Oc
0.032
0.030
0.028
0.026
0.024
0.022
0.020
-5 -4 -3 -2 -1 0 1 2 3 4 5
Canard Offset
Incidence = 2.5 deg

(a)

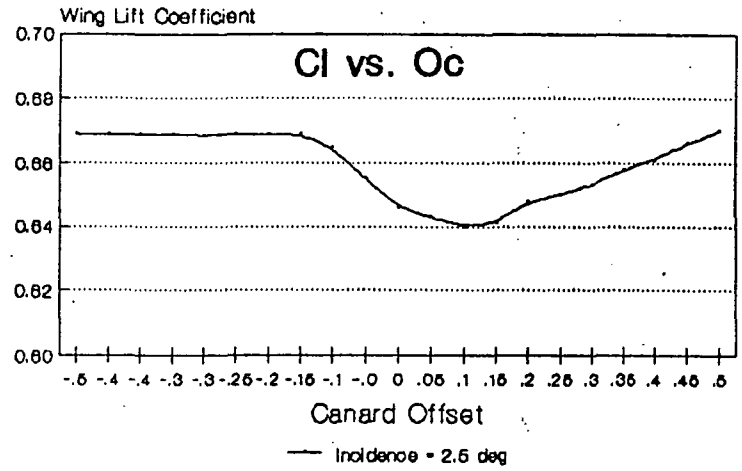
Wing Lift Coefficient
Cl vs. Oc
0.70
0.68
0.66
0.64
0.62
0.60
-.5 -.4 -.4 -.3 -.3 -.25 -.2 -.15 -.1 -.0 0 .05 .1 .15 .2 .25 .3 .35 .4 .45 .5
Canard Offset
Incidence = 2.5 deg

(b)

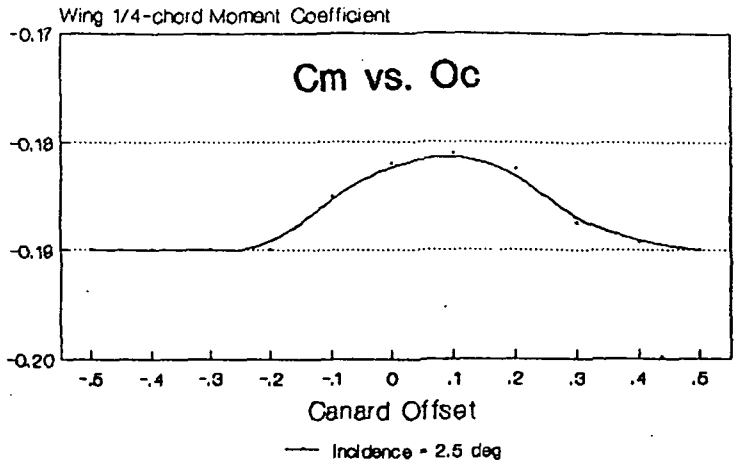

(c)

Figure 8: Trade-off Studies for Wing Placement

Drag

The total airplane drag consists of skin friction, form, induced, interference, trim, and cooling drag. All of the parasitic drag coefficients were calculated using the respective wetted areas with an equivalent skin friction coefficient, Cf = .0045.

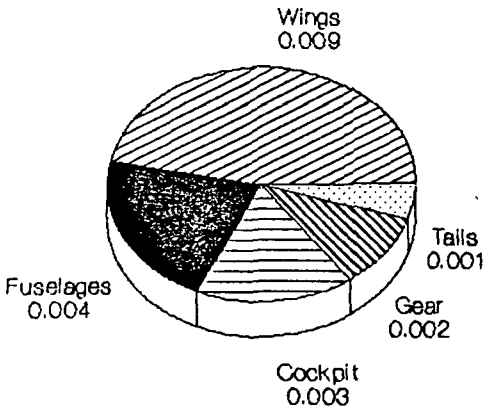

Figure 9: Parasitic Drag Breakdown

The total drag coefficient for the Gryphon is C_D = .0145 + .021*C_L^2. This seemingly low induced drag coefficient is due to the tandem wing configuration's theoretical 50% drag

reduction, found in Reference 12. A CD_0 of .0145 will be maintained by smooth skin conditions and close tolerances on interfering components. These low drag coefficient values could be a bit optimistic, but actual values will not vary by more than 20%. The total drag build-up can be seen in Figure 10.

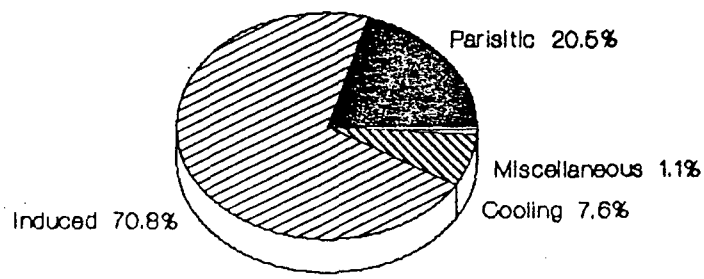

Figure 10: Total Drag Buildup

STRUCTURES

Material Selection

The major structural material needs to be both high strength and low density. Metal materials are too high in density for their strength. Therefore, composite materials were chosen. Composite materials are also stiff enough to prevent the wings from deflecting too much and scraping the runway.

The major structural material selected for the Gryphon was Graphite fibers in a Polyamide-imide matrix (Gr/PAI). This material was selected over Graphite/Epoxy (Gr/Ep) due to its higher strength, corrosion resistance, and impact resistance. In places were these properties are not needed, Gr/Ep is used to reduce cost. Gr/PAI was chosen over Kevlar/Epoxy due to Kevlar 49's low compressive strength which was found to be the key design parameter for the materials chosen.

To further decrease the weight of the plane and increase the stiffness, Nomex honeycomb will be used. Characteristics for the main materials used are shown below.

Table 1: Material Properties

	Compression (psi)	Modulus (psi)	Density (in/lb^3)
Graphite/PAI	95	10	.056
Graphite/Epoxy	30	2.3	.056
Nomex Honeycomb	.81	.045	.0017

Wing Structure

To analyze the wing structure, the spar was divided into 3 foot sections. Maximum loads were placed on the wing concentrated at the center of these three foot span sections as shown in Figure 11. From the moments produced by the loads and the stress the material could handle with a Safety Factor of 1.5, the moments of inertia for each section were found. Using the moments of inertia, the dimensions of the spar were found through interpolation.

The center section of the wing was designed to handle the added compressive forces encountered when the twin fuselage are not balanced with respect to each member. The front center section holds all the fuel for the plane as shown in Figure 12.

The wing box is designed to transfer all loads and torques to the spar and thus does not carry large loads or torques. The ribs are spaced three feet apart, corresponding to the designed load concentrations. The skin, ribs, leading and trailing edges are shown in Figures 13 and 14.

For the added torque and loads created by the engines on the back wing, the ribs' skin thickness is increased nines times the thickness of the rest of the ribs. The spar through that section of the wing to which the engine is mounted is shaped as the spars through the center section of the wings as shown in Figure 15. Besides these sections, the structure and

size of the back wing are the same as the front.

The front wing has the addition of the elevators for pitch control and cooling channels through the upper and lower skin as shown in Figure 12.

The cruise wing deflection was estimated to be two feet. The maximum wing deflection was calculated to be 6 feet at the maximum load factor of 2.5.

Fuselage and Vertical Tail Structure

The structure of the fuselage and vertical tail are shown in Figure 16. Most of the fuselage is unused and designed around ground clearance and aerodynamic considerations. The largest known load on the fuselage is that from the vertical tail. The maximum possible load from the vertical tail was used to analyze the beams used to make the frame of the fuselage. The beam could handle the loads placed on it from the tail.

The structure of the vertical tail was analyzed in the same manner as the wing. The structure of the spar is the same configuration as the spar for the wing carry through except there is no foam filling the hollow center. The outer half of the spar is designed with the same configuration as the beams that form the structure of the fuselage.

LOADS ON WING

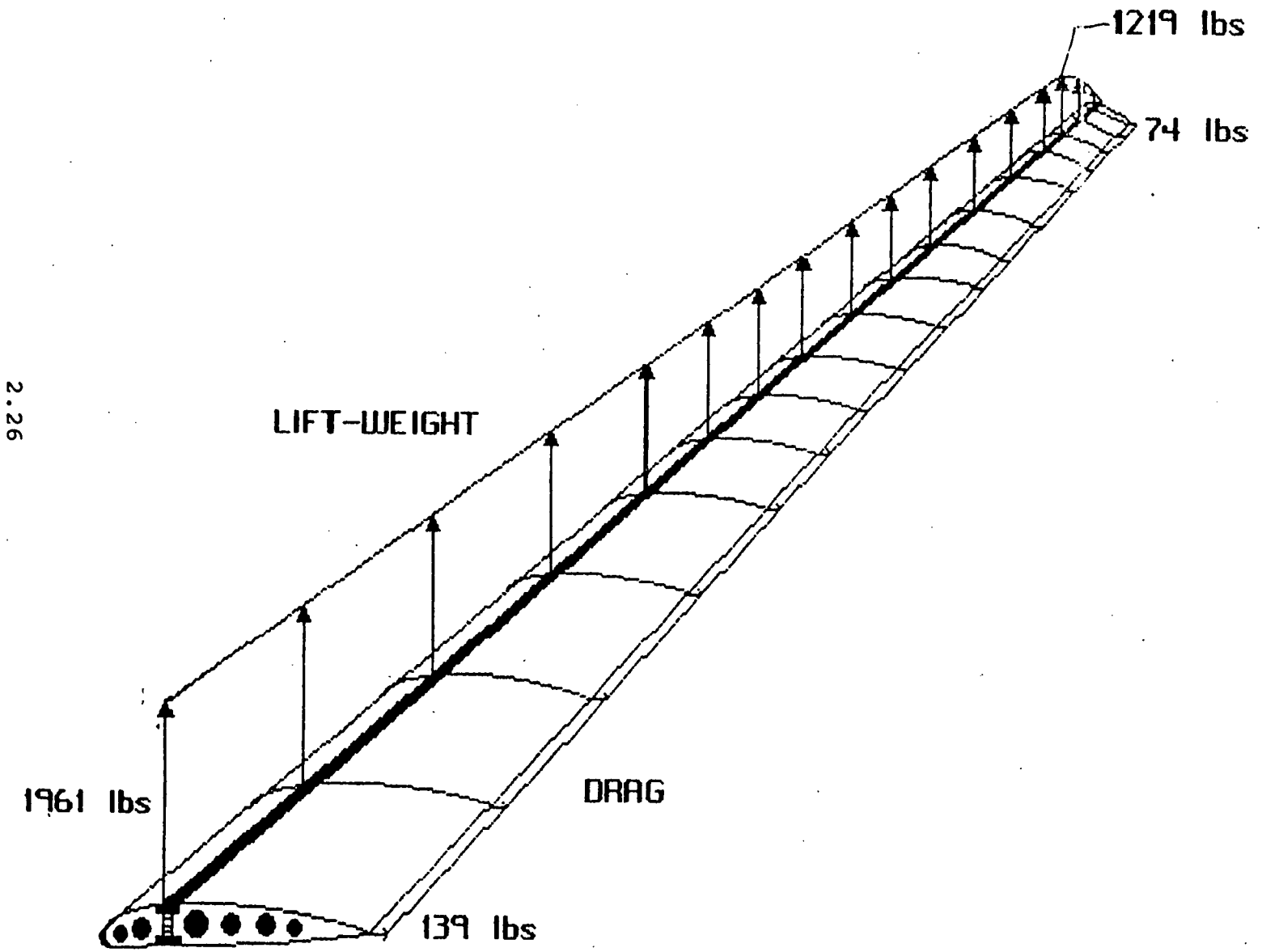

2.26

Figure 11

FRONT WING

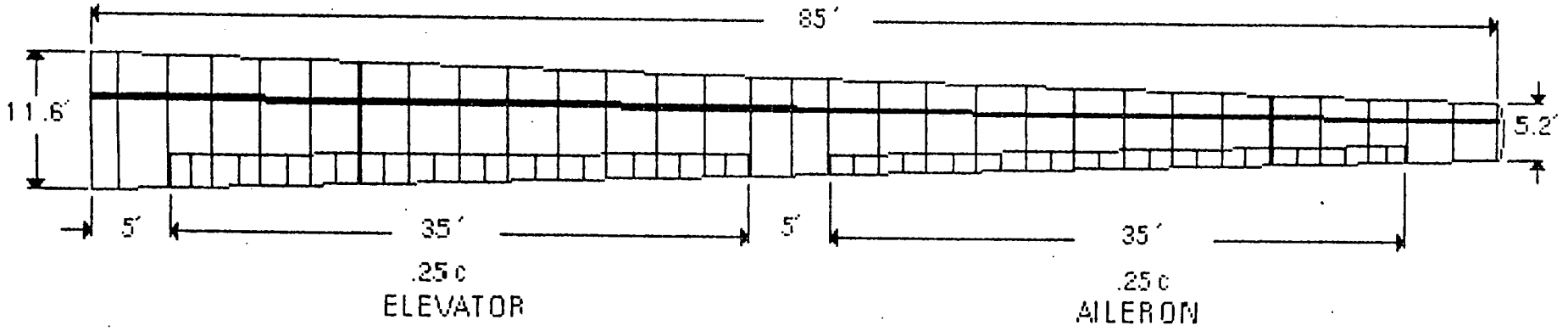

OUTBOARD SECTION

2.27

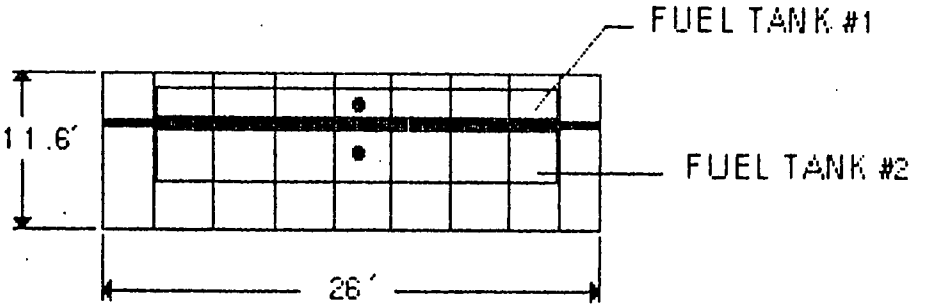

CENTER SECTION

Figure 12

CENTER WING CROSS-SECTION

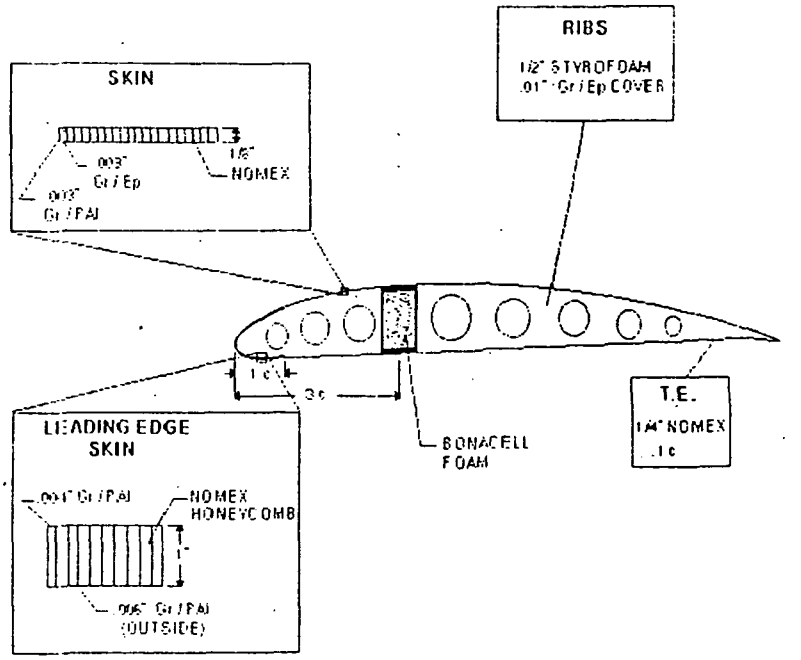

Figure 13

OUTBOARD WING CROSS-SECTION

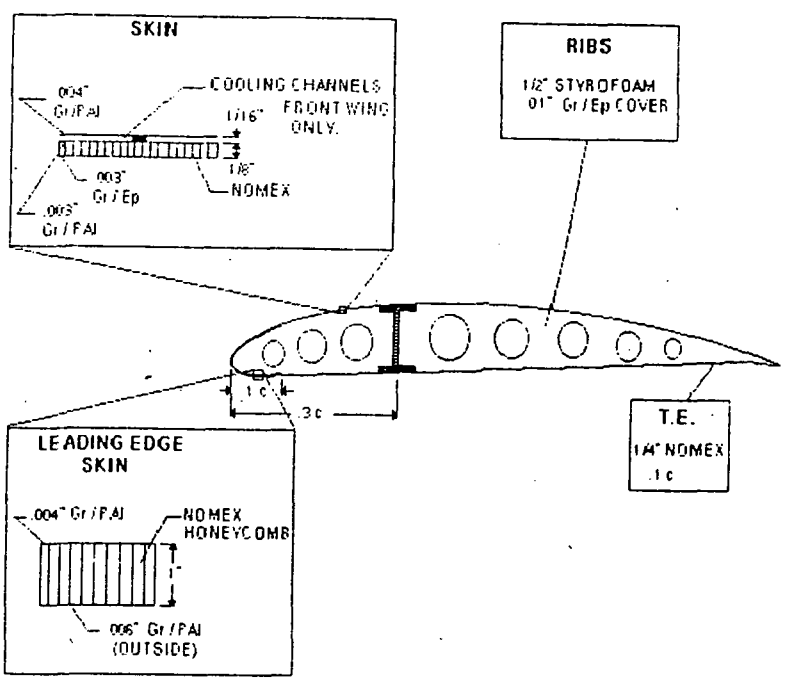

Figure 14

REAR WING

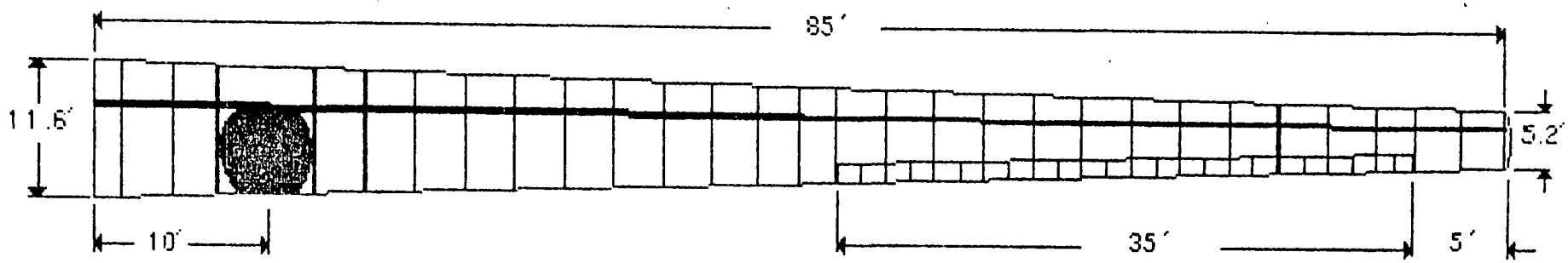

ENGINE PLACEMENT
ON WING
AIR INTAKE ON
BOTTOM OF WING

.25c
AILERON

OUTBOARD SECTION

2.29

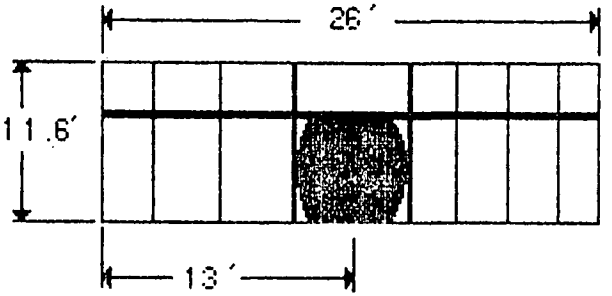

CENTER SECTION

Figure 15

STRUCTURE OF FUSELAGE AND V. TAIL

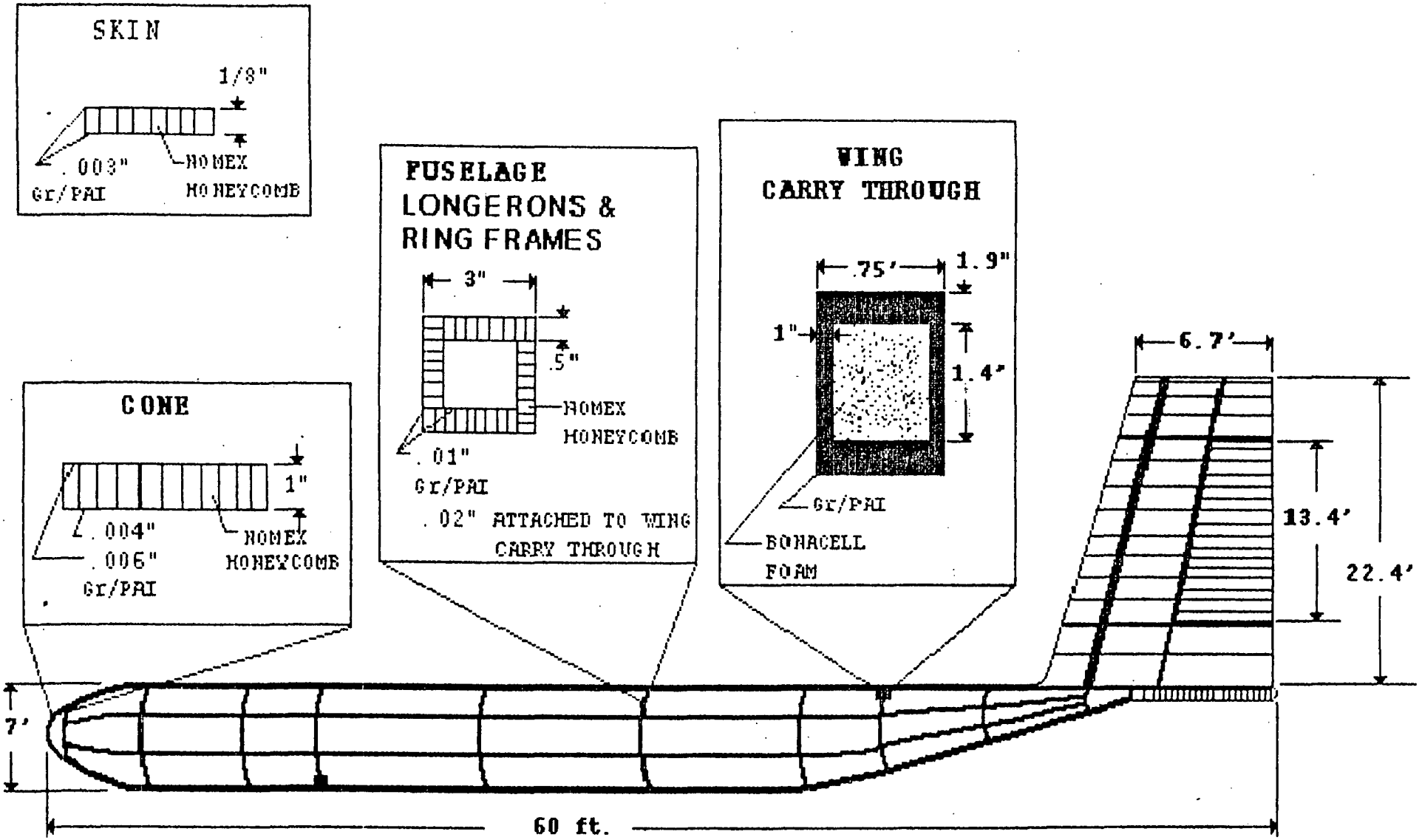

Figure 16

LANDING GEAR

The design of the landing gear presents many problems. The landing gear must be placed in the correct down position for landing, and must somehow retract and fit into the aircraft structure. The layout of the landing gear is shown in Figure 17.

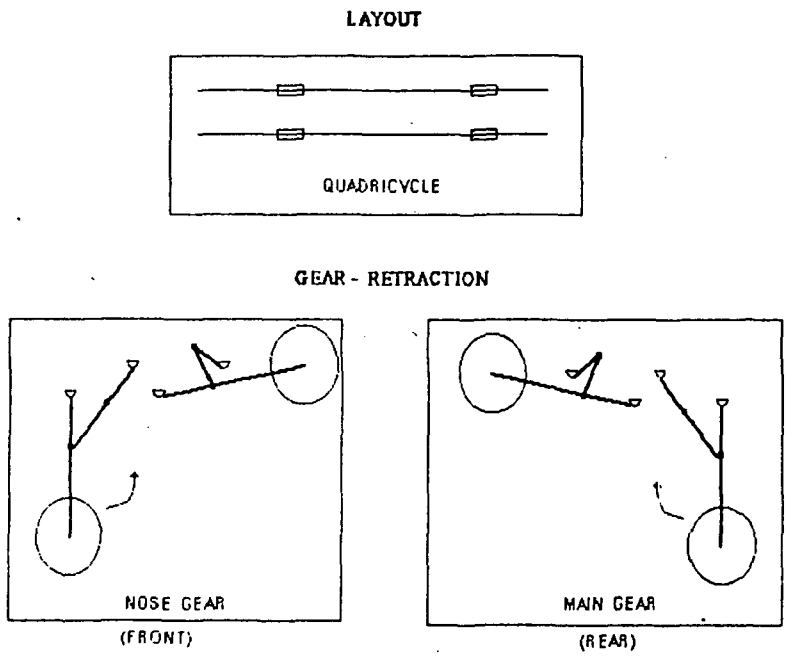

Figure 17: Landing Gear Geometry

This layout permits the retraction of the landing gear into the twin fuselage. The elliptical shape of the fuselage helps in reducing the length of the landing gear. If the main gear was placed on the high back wing (see Figure 18), the length of the landing gear would have reached a minimum of about 12 feet. With the landing gears on the elliptical

fuselage, the length is reduced significantly from 12 feet to 4.5 feet. Another advantage in placing the landing gear on the fuselage instead of the wing is the reduction of the huge bending moment resulting from the long landing gear.

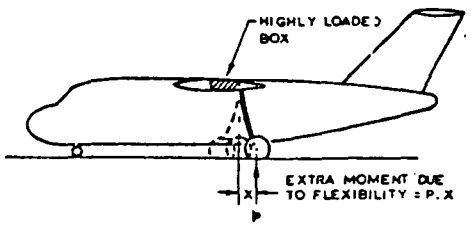

Figure 18: Landing Gear on High Back Wing (Ref. 3)

Designing the landing gear consists of tire sizing, tire selection, stroke determination for the shock absorbers, and choosing the material.

Tire Sizing

As seen in the drawing in Figure 19, the tire sizing calculation was performed. Table 2 shows the loads on the tires.

Table 2: Tire Loads

Maximum Static Load	22,900 lb
Maximum Static Load (nose)	5,600 lb
Minimum Static Load (nose)	2,800 lb
Dynamic Braking Load (nose)	1,054 lb

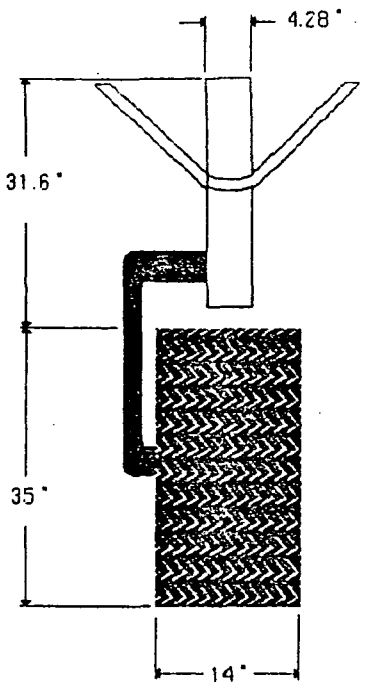

Figure 19

Tire Selection

With the required load on the tires calculated, the tire selection can be made. Table 3 lists the information for the tire selected.

Table 3: Tire Selection Information

	Main Gear	Nose Gear
Tire Type	Type VIII	Type VIII
Size	37 x 14 -14	28 x 9 -12
Max. Speed	225 mph	156 knot
Max. Load	25,000 lb	16,650 lb
Pressure	160 psi	235 psi
Max. Width	14 in	8.8 in
Max. Diameter	37 in	27.6 in
Rolling Radius	15.1 in	11.6 in

Shock Absorbers

The type of shock absorber used was the oleo shock-strut. The stroke determination and oleo sizing are shown in Tables 4 and 5.

Table 4: Stroke Determination

	Main Gear	Nose Gear
Stroke Determination	12.5 in	12.65 in

Table 5: Oleo Sizing

Length	Diameter
Main Gear = 31.25 in	Internal = 4.02 in
Nose Gear = 31.62 in	External = 4.28 in

Material Selection

Material selection was based on weight saving, thus a composite material was chosen. The composite material is Graphite Polyamide-imide. The composite has a compressive stress of 63,000 psi (with safety factor included), and the values for tensile and flexural stresses are even higher.

PROPULSION

Engines

Several of the design drivers for this project were related to the propulsion system required for the airplane. One of the most important aspects of the missions is that the density at 100,000 feet is so low that most air-breathing engines can not compress enough air to maintain power. Another design driver is the fact that the plane must have a low structural weight. This means that the power to weight ratio for the engine must be large. The propeller must have a high efficiency rating in order for the airplane to have as much power available as possible.

Several different types of engines were researched, hoping to find one that would meet the requirements. The turbofan and turbojet engines were found to lose power proportionately with the altitude. While the turbojet could be enlarged to increase the combustion chamber, it was found that in order to reach 100,000 feet, the size of a regular turbojet would have to increase 100 times. This could not meet the weight or size requirements.

Both liquid and solid rocket engines were investigated, but they were found to have a very high specific impulse, which would be detrimental to the low structural weight of the aircraft. If an engine was used that had a low specific impulse, there wouldn't be enough power to reach and maintain

altitude, without using several small engines. Again, this would defeat the weight requirement.

Another option for a propulsion system that was not used was the idea of using microwave or laser technology to power the craft. Microwave propulsion would not be feasible because the beam to the airplane would be unsafe for the environment and other airplanes in the area. The laser would be difficult to operate because there are currently no satellites available that could reach all areas of the Earth, especially the entire distance from the equator to the South Pole. Also, this is unproven technology, and the airplane will be unmanned for some missions. This runs the risk of being a potential hazard.

There were two alternatives that were the most popular ideas for powering this plane. The first one was solar power. Most of the atmospheric particles can be found below 100,000 feet. Therefore, there are more than enough solar rays to power an airplane of this size. However, the plane would only be able to fly in the lower atmosphere during daylight hours because of the reduced solar power available. The weight of the solar cells on the wings is also of major concern to the structural weight. The wings could not support their weight efficiently. Furthermore, the price of the most efficient solar cells, gallium arsenide, is too high. To build just 2 experimental airplanes, the cost would be unreasonable. The

other idea for a propulsion system was to use hydrazine in the engine. When reaching 100,000 feet, the hydrazine could be run through the engine instead of the fuel. This monopropellant could work as a coolant, as well as a fuel. This proposal is good, but hydrazine is toxic and dangerous to work with. Using it in an unmanned craft might not be a good idea. Also, the weight of the hydrazine would increase the weight of the plane too much to make the extra power very effective. This weight constraint also prohibits bringing oxygen up in the plane to be used in conjunction with another engine to increase the combustion power. Pumps would be needed to reach the necessary compression, and all of this equipment would weigh too much.

The final decision for a propulsive device was the internal combustion engine. Most of these have a high power to weight ratio, and their power can be increased with the use of turbo- or superchargers. The one that was found that met the requirements the closest was the Teledyne Continental GTSIOL 550 engine with three stages of turbocharging. Currently, with two stages of turbocharging, the engine can produce about 400 horsepower at 70,000 feet. Teledyne has been researching the use of a third turbocharger, and has found that at 100,000 feet, the engine should be able to produce 400 horsepower. Figure 20 shows a schematic of the engine with some of its specifications. The low specific fuel

consumption was an important factor in the engine determination because it would require less fuel than most other internal combustion engines.

TELEDYNE CONTINENTAL
GTSIOL 550

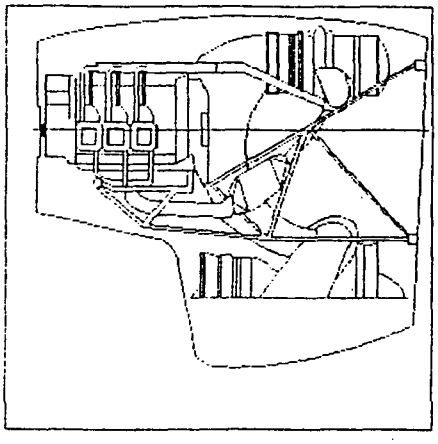

GTSIOL 550 WITH 3 STAGES OF TURBOCHARGING

SPECIFICATIONS	
HEIGHT	33.5"
WIDTH	42.5"
LENGTH	42.64"
WEIGHT	1900 lb.
RATED POWER	500 HP
BSFC	.45 lb / HP / hr

Figure 20 (Courtesy of Teledyne Continental)

Propellers

In order to make the available power as useable as possible, a propeller needed to be found that would not only be able to operate in the low Reynolds number regime, but that would also have a high efficiency rating. The advanced propfan was found to have a much higher efficiency than a regular propeller. The propfan that is shown in Figure 21 will be implemented on the Gryphon.

PROPFAN SPECIFICATIONS

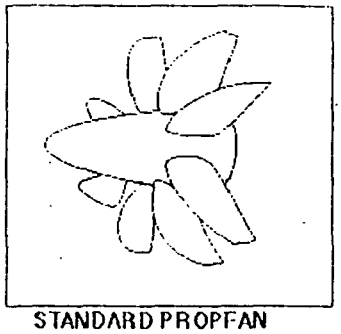

STANDARD PROPFAN

DIAMETER = 16 feet

BLADES = 8

EFFICIENCY = .90

SPAR-SHELL CONSTRUCTION

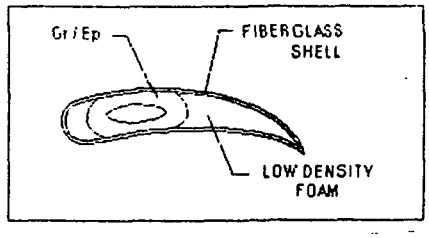

Figure 21

The propfan diameter required to produce enough power at 100,000 feet was calculated as being 16 feet. While this is longer than the current propfan blades, the efficiency can still be maintained at around 90%. There will be eight blades on the propfan, and the blades will be of variable pitch, in order to maximize the efficiency in all flight regimes.

In order to reduce the weight of the propfan, the blades must be designed with a lightweight material. The material must be strong, and the structure of the blade must be sturdy. The design that was chosen as most efficient for the propfan was the spar-shell configuration. The shell will be made of fiberglass, a composite with a high allowable fatigue to modulus of elasticity ratio. The spar should be made of a material with a similar modulus of elasticity so that it the blade will be structurally sound in different temperature

regimes. A graphite/epoxy composite was chosen for this material. Figure 21 shows the basic construction of a propfan blade. The low density foam used in the cavity will help distribute the loads evenly across the blade, without a large weight gain.

Engine Cooling

Again the low densities involved in flying at altitudes exceeding 80,000 feet considerably limit the design of the airplane and its subsystems. Conventional airplane cooling techniques prove worthless when dealing in the low Reynolds number regime. The size of a conventional engine/component cooling system needed to effectively reject the necessary heat produced by the engine and its subsystems would cause the total drag of the airplane to double in magnitude. The effect of flying at high altitudes serves a design advantage, however, in that the surrounding freestream air is frigid (T = -35 degrees F). The design of the cooling system was influenced in a major way by the low temperature freestream conditions and by the fact that the High Flyer would have a huge wing surface area.

Methods for cooling at low Reynolds numbers are varying. Some attention should be given to each method with a list of advantages and disadvantages:

Using the Fuel as Coolant with Wings as Radiators

WING AS HEAT RADIATOR

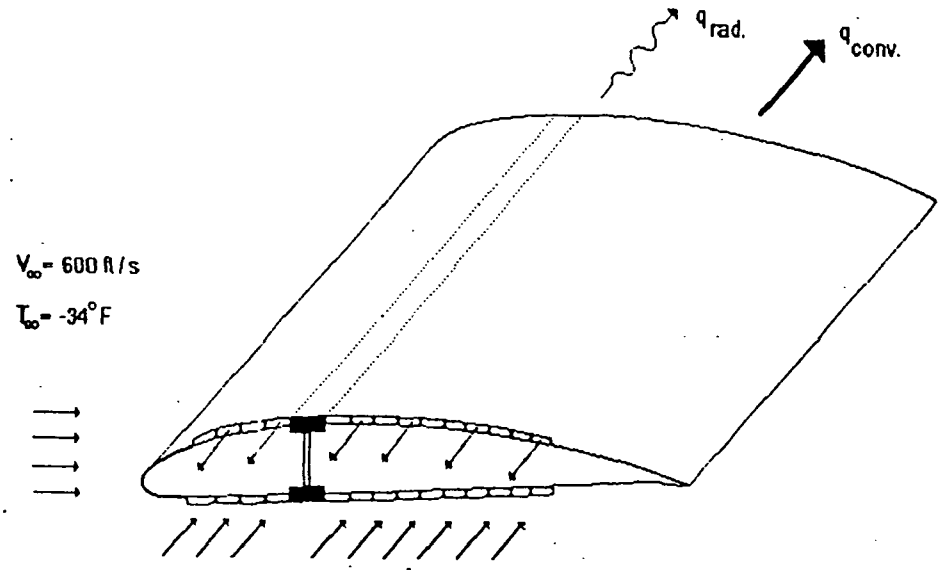

Figure 22

This is one of the more promising heat transfer ideas because of the possibilities of cooling with very low drag penalties. Problems arising from this configuration include vapor lock, a low heat transfer coefficient of the skin, and high structural weights. The latter two problems can be solved by finding a material which will be able to conduct heat effectively while offering a high strength to weight ratio. Some promising material alternatives are Graphite/Epoxy, Graphite Polyamide-imide, and Kevlar. The vapor lock problem can be easily avoided by placing fuel pumps in areas where the fuel/coolant is in a liquid phase, such as at the front wingtips and at the intake side of the engine.

Liquid Cooling with Conventional Radiators

This offers much in the way of reliable engine cooling without the possibility of overcooling. The required size of the radiators becomes extremely large at altitudes exceeding 100,000 ft. This causes the cooling drag to account for 75%

of the total drag on the airplane. Therefore, this method is unacceptable.

Oil Coolant Radiators

If used by themselves the amount of oil to be carried on a particular mission would far outweigh the advantages of using oil as a coolant. Oil coolant radiators can be used effectively with other forms of cooling systems.

Using the Fuel Tanks as Stores of Coolness

This method would involve the use of a liquid coolant such as water. It would pass this coolant into the fuel reservoirs to lower the temperature by a precooled fuel volume. This is a very promising alternative to using the fuel/coolant in the wings. Its major drawback is that it cannot be the only means of cooling since the most demanding heat transfer phase of most of the missions specified in the RFP occurs beyond the halfway point. This means that the fuel's cooling capability would be somewhat diminished by the time it reached its most critical point.

Hydrazine Internal Combustion Engine

This solves the problem by relying on a monopropellant as a fuel in an alternate engine. Hydrazine is toxic and the extra weight needed to carry the necessary monopropellant and extra engine cannot be afforded.

Heat Recycling in a Steam Turbine

Using water as the cooling medium, route the heated

supply into a steam turbine to effectively dissipate and harness the medium's heat energy. The internal combustion engine does not currently operate at temperatures greater than 500 (deg. F). Current steam turbines require mean steam inlet temperatures 500 (deg. F) and greater. Since the coolant temperature should be much lower than the engine's operating temperature to effectively conduct heat, this method is not currently advisable. This method could be reconsidered if an engine were designed specifically for this purpose with thin walled cylinders. These special cylinders could heat up to combustion temperatures (3800 deg. F) allowing the free passage of heat from the cylinder to the cold side steam supply. Since a strap-on engine was desired for this project, this idea was not integrated into the design.

Keeping these ideas in mind, an energy efficient method of cooling the three engines at high altitudes was devised. A cooling system was designed based on three subsystem coolers that, through their combined effect, facilitate the necessary heat rejection at altitude. The major subsystem consists of a thin-walled passageway along the skin of the wing in which fuel is used to convect heat to the outer wall, from where convection forces the heat into the freestream, as shown in Figure 22. This fuel will not be available to the engine for propulsive matters, but the volume is so small that the additional weight is negligible to the overall airplane

weight.

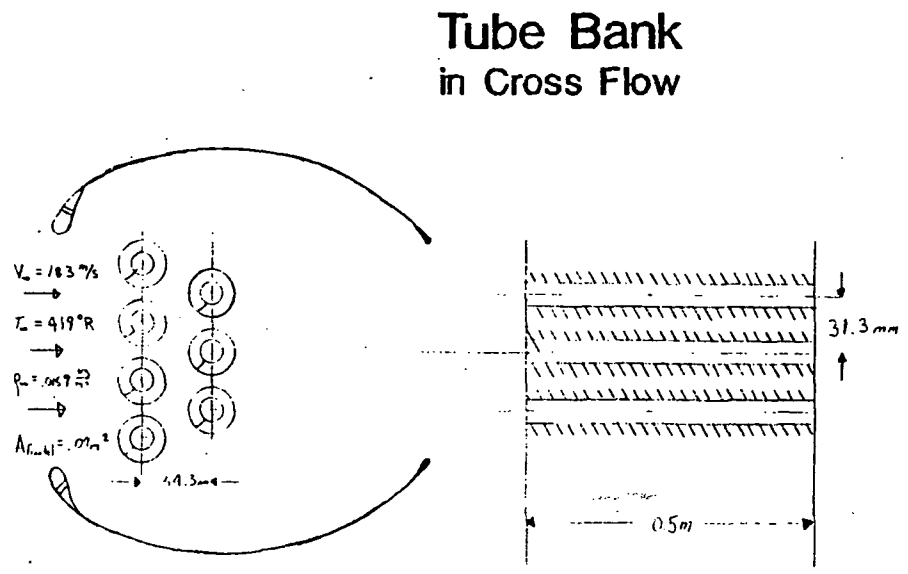

Figure 23

The second subsystem consists of oil coolers placed around the cowling of the engine. The oil cooling radiator is a finned tube bank in cross flow with the freestream, designed specifically for maximum cooling with a minimum cooling drag (Figure 23). Each GTSIOL 550 engine is equipped with its own oil cooling device, rejecting 40 kW of heat each with a combined drag coefficient of only .0012. The third cooling subsystem is a unique design aimed at increasing the overall efficiency of the engine at its design altitude. Since the fuel is used as a coolant, a good way to reject excess heat is to burn the fuel directly after it has absorbed a sufficient amount of heat from the engine. This process will increase the engine's operating temperature, helping to increase the

efficiency of the engine. This energy scavenging system allows the additional rejection of 100 kW of heat.

Using the fuel as a coolant increases the possibility of vapor lock, which is common to engines in which the fuel lines are in close proximity to the exhaust manifold. Either the fuel will be pressurized in the coolant passageway at 35 psia and at its highest temperature of 351 deg. K, or electric fuel pumps will be placed at the wingtips to circumvent this problem by pumping the fluid once it is well below its vaporization temperature.

FUEL/COOLANT SYSTEM CONFIGURATION

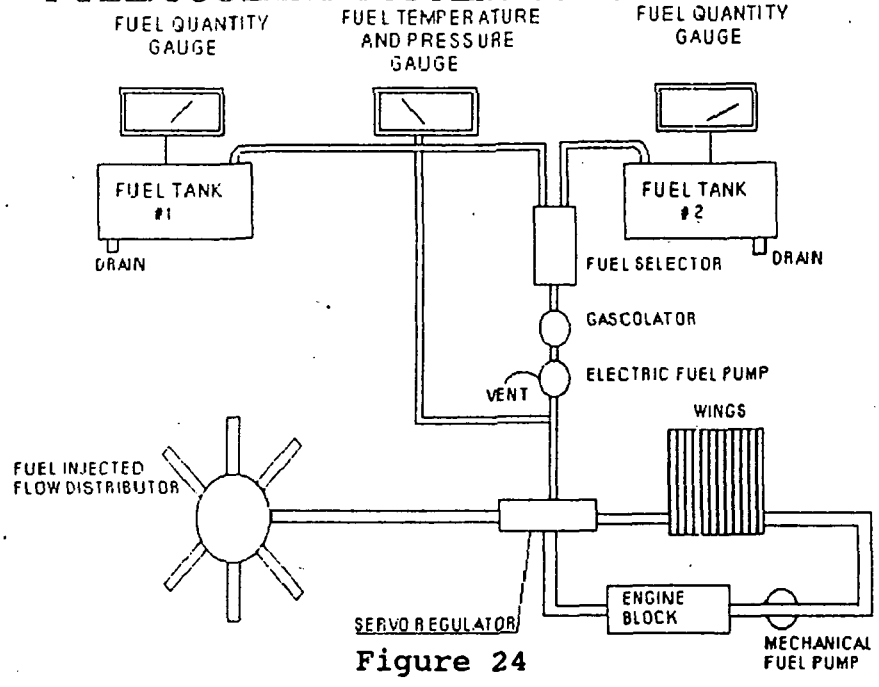

Figure 24

The use of three mechanical fuel pumps placed immediately before the engine cooling jacket inlet further reduce the possibility of vapor lock.

In order to validate the use of fuel as a cooling medium,

it was necessary to conduct a heat transfer analysis of the cooling properties of Aviation Fuel 110/115 across the cylinders of the engine block. The power plant is a horizontally opposed 550 cubic inch fuel-injected engine, which means that there are three cylinders per engine face (Figure 20). Given the 4 inch cylinder stroke and the 2.7 inch cylinder bore, the total cooling surface area can be calculated as 2076 square inches. Using the inlet and outlet temperatures from the wing's radiators (T_{in} = 309 deg. K and T_{out} = 351 deg. K), the convective heat transfer coefficient was calculated, using the Zhukauskas Relation and Churchill's Relation, as 996 W/m^2-K for a cylinder in cross flow. This agrees with Newton's method for defining the convective heat transfer coefficient, which simply states that it is a function of surface area, heat produced = 300 kW, and temperature difference, h= 1000 W/m^2-K.

The performance analysis for the Gryphon was conducted using methods derived from References 1, 13, and 15. The main parameters used in the analysis are found below in Table 6. The mission requirements are summarized in Figure 25. A summary of the overall aircraft performance is found in Table 7. The constraint diagram is found in Figure 26. Unless otherwise stated, all calculations are based on the aircraft configured for the primary mission (Mission #1).

PERFORMANCE PARAMETERS

Wto = 26000 lbs (mission 1,2 and 3)
Wto = 20000 lbs (mission 4)

Sw = 3400 ft2
AR = 12 (effective)
e = .631
Cdo = .015

prop efficiency = .9
max rated Power = 1200 hp (at 100,000 ft)
max rated Power = 1500 hp (sea level)

CLmax = 1.45

Table 6

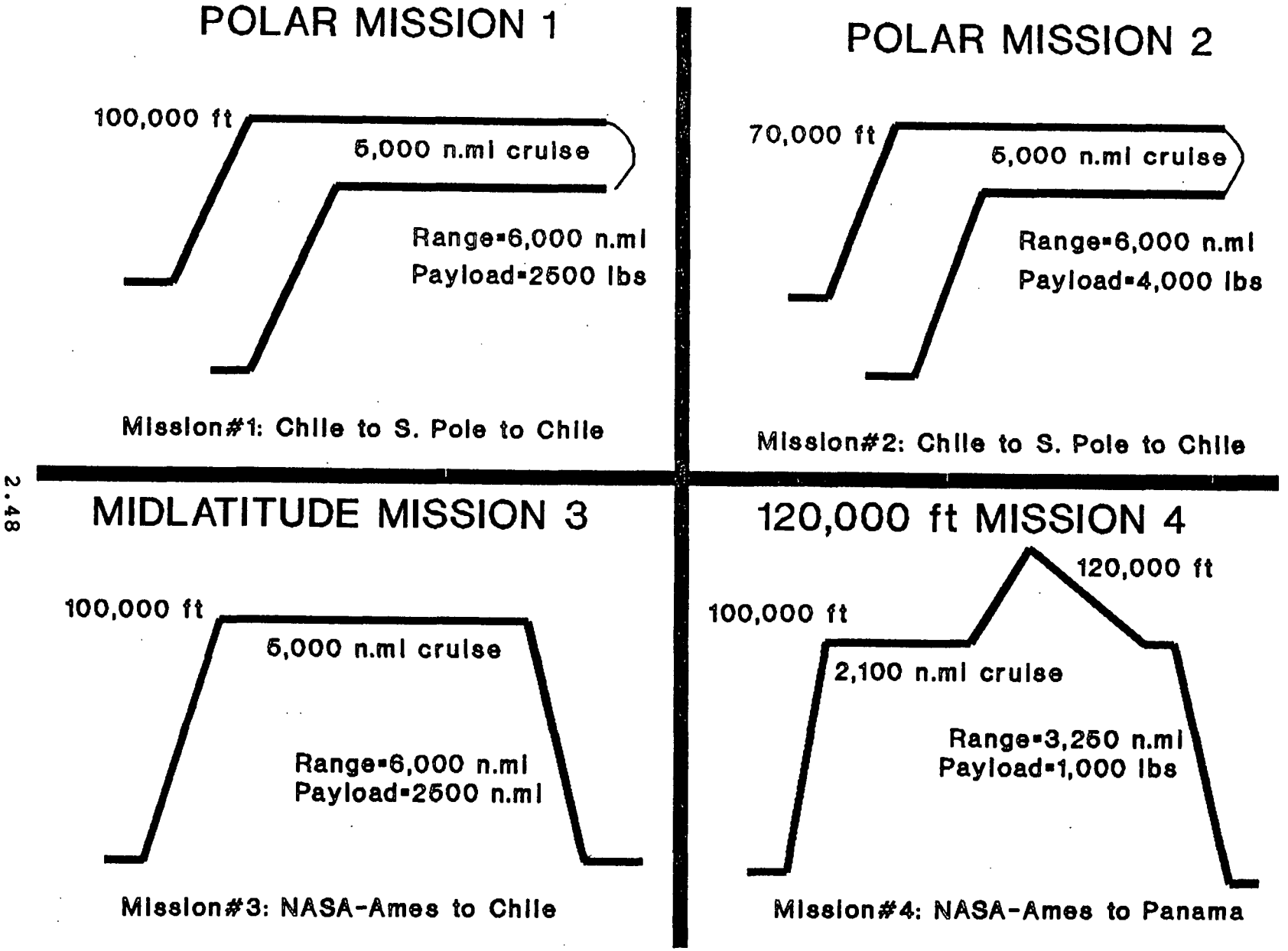
POLAR MISSION 1
100,000 ft
5,000 n.mi cruise
Range=6,000 n.mi
Payload=2500 lbs
Mission#1: Chile to S. Pole to Chile
POLAR MISSION 2
70,000 ft
5,000 n.mi cruise
Range=6,000 n.mi
Payload=4,000 lbs
Mission#2: Chile to S. Pole to Chile
MIDLATITUDE MISSION 3
100,000 ft
5,000 n.mi cruise
Range=6,000 n.mi
Payload=2500 n.mi
Mission#3: NASA-Ames to Chile
120,000 ft MISSION 4
120,000 ft
100,000 ft
2,100 n.mi cruise
Range=3,250 n.mi
Payload=1,000 lbs
Mission#4: NASA-Ames to Panama

Figure 25

GRYPHON PERFORMANCE

TAKEOFF	825 FT @ Vto = 79 fps rotation angle = 15 degrees
LANDING	1760 FT @ Vapproach = 86 fps
RANGE	8250 n. miles
ABS CEILING	100,000 ft (Mission #1,2,3) 110,000 ft (Mission #4)
LIMIT LOAD FACTOR	3.75

Table 7

CONSTRAINT DIAGRAM for GRYPHON

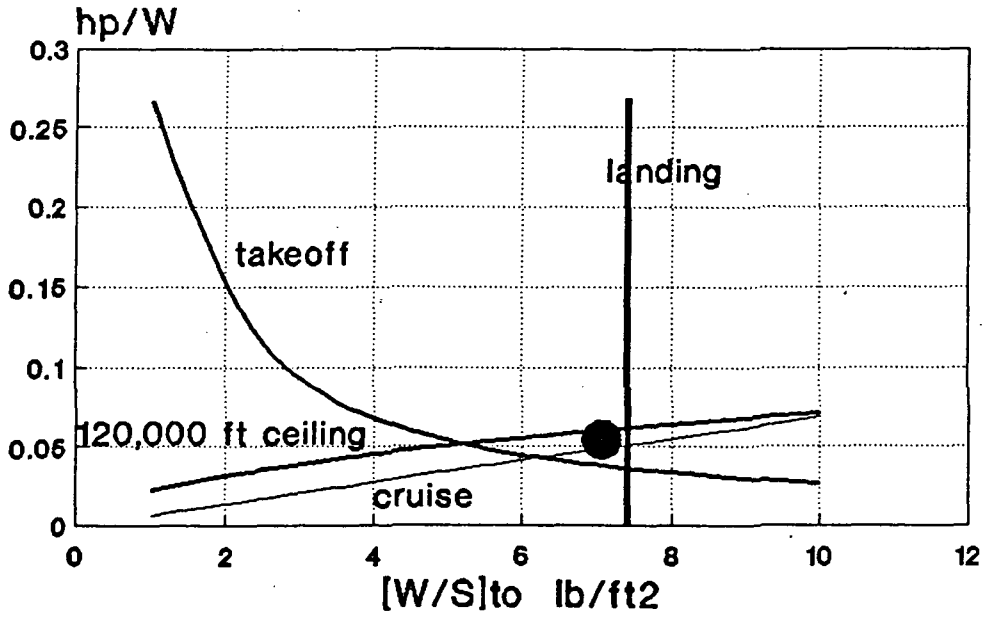

Figure 26

Takeoff and Landing

For the takeoff and landing analysis, it was assumed that the altitude of the runways are at 5,000 feet. Using the FAR 23 takeoff specifications with a 50 foot obstacle, the takeoff distance for the Gryphon was 825 feet. This is at a takeoff velocity of 79 fps and takeoff CL of .8(CLmax). The rotation angle was 15 degrees. To prevent the pusher props from brushing the ground, the rotation angle should be kept at less than 19 degrees. The landing gear length was sized to 5.5 feet to clear the 4 foot high obstacles in the runway. Ground effects during takeoff were not considered in this analysis.

The landing distance for the Gryphon was 1760 feet. The approach speed and angle was 85.35 fps and 2.2 degrees, respectively. This was analyzed with half the fuel remaining during landing. The landing CL was .8(CLmax).

Since the engine cooling panels were located along the wing span, spoilers could not be employed on the Gryphon. Instead, the aileron and flap combination would be used as the alternative lift dump device.

V-n Diagram

The aerodynamic loadings experienced by the Gryphon is illustrated in Figures 27 and 28. Since the Gryphon will not be required to do any difficult maneuvers, the gust loads will be the dominating factor in determining the

V-n Diagram at
Cruise Conditions

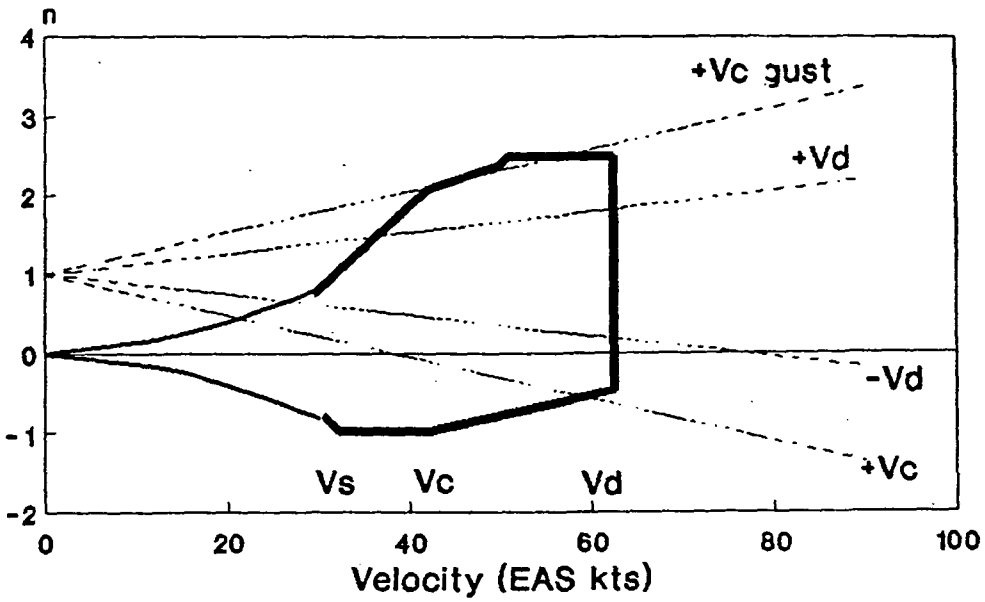

Figure 27

V-n Diagram
at Low W/S Landing

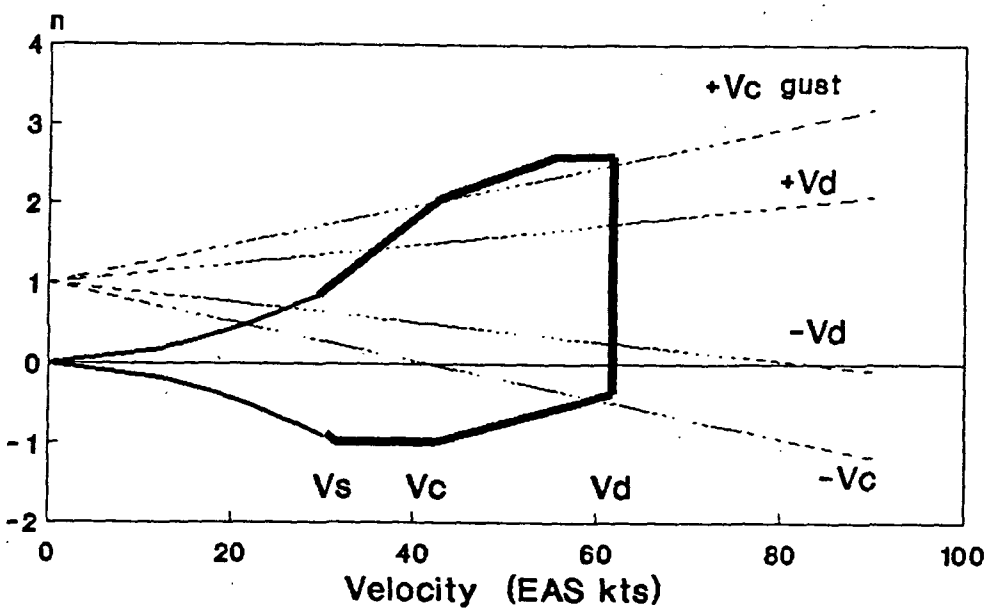

Figure 28

ultimate load factor of the aircraft. From Figure 27, the gust loads during cruise were within the FAR 25 maneuvering limit load factors of 2.5 and -1. The gust intensities used at the cruise and dive speeds were 12 and 6 fps , respectively.

The worst case loading for the Gryphon occurred during gusty landing conditions (see Figure 28) and with no fuel remaining. Again, the gust loads were found to be within 2.5 and -1. The gust intensities used for this analysis were 50 and 25 fps.

The ultimate load factor for the Gryphon was chosen to be 3.75 and -1.5. These factors include the 1.5 safety factor over the FAR 25 limit load factors.

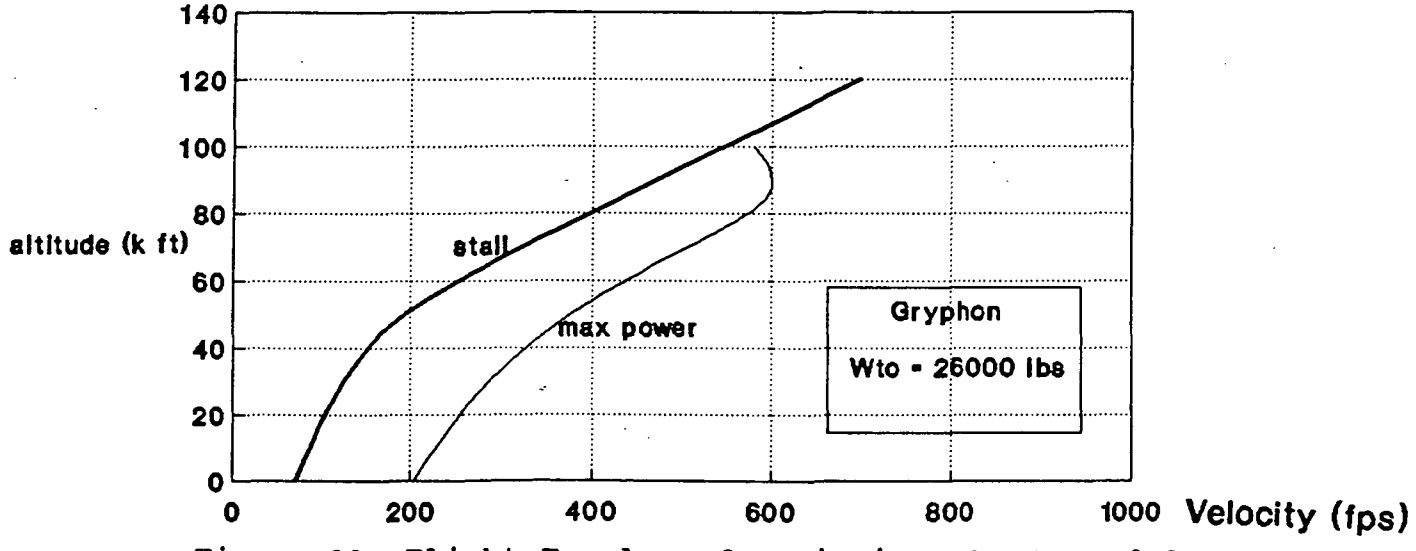

Figure 29: Flight Envelope for Missions 1, 2, and 3

Flight Envelope (Missions 1, 2, 3)

Figure 29 represents the flight envelope for Missions 1,

2 and 3. The absolute ceiling is 100,000 feet and the maximum velocity is 600 fps. The stall speed at 100,000 ft is 540 fps. From these initial restrictions, the Gryphon does seem to meet the specified cruise requirements.

Mission Flight Paths

Climb Profile

Using energy-state approximation methods, a minimum fuel-to-climb trajectory was chosen to minimize the weight of the aircraft (see Fig. 30). The climb profile was designed to have a 10% margin over stall speed for safety. The time-to-climb to 100,000 feet was found to be 1.7 hours. The fuel consumed was 1200 pounds. The time-to-climb to 70,000 ft was 1 hour with a fuel consumption of 800 lbs.

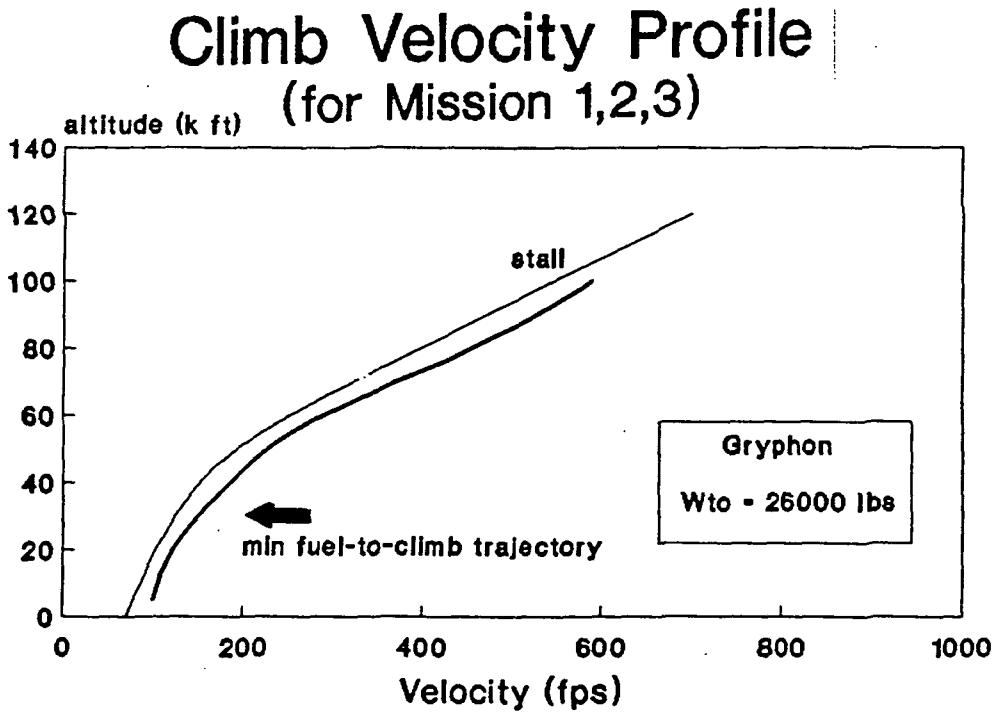

Figure 30

Cruise Profile

Figure 31 represents the power requirements during cruise for Mission 1. At the beginning of the cruise leg, 97 percent of the power available is needed. As fuel is consumed, the power requirements are reduced. Halfway through the cruise leg, the power requirement was down to 80 percent.

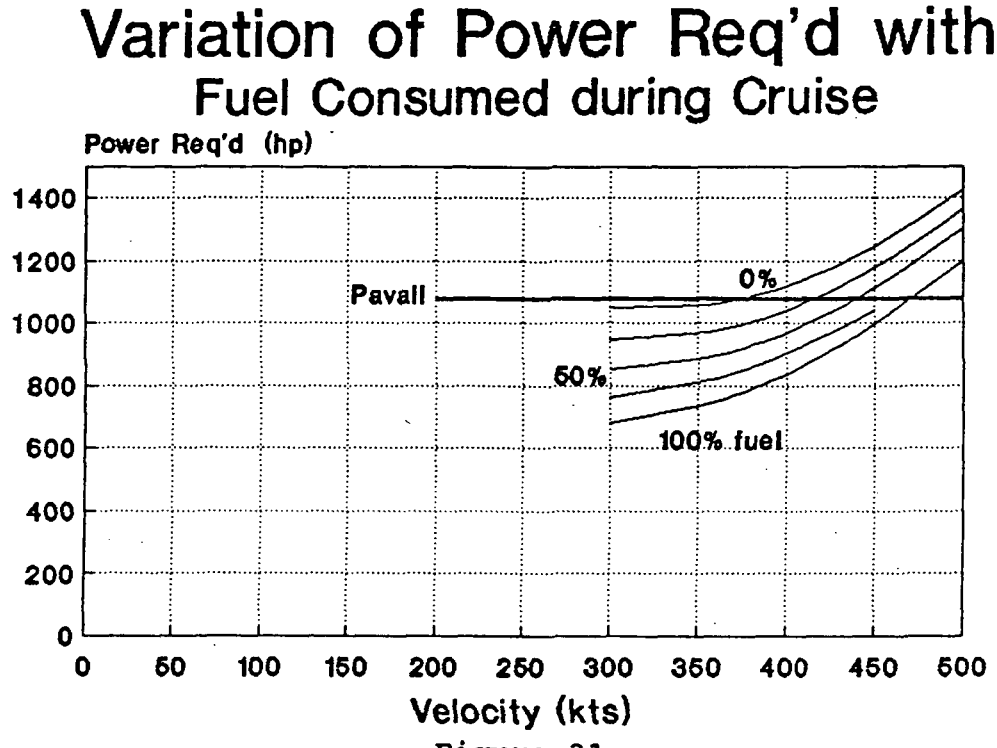

Figure 31

Table 8 shows the cruise profiles of each of the 4 missions. These cruise points were determined for maximum range, which results in a lower takeoff weight.

	#1	#2	#3	#4
Mach #	0.57	0.35	0.57	0.57
CL	1.3	0.7	1.3	0.96
AoA	7 deg	3 deg	7 deg	5 deg
Preq'd	864 hp	460 hp	864 hp	759 hp
Fuel	6300 lbs	5020 lbs	6300 lbs	1900 lbs

Table 8: Cruise Profile per Mission

On a side note, the effect of angle of attack on the tandem-wings was investigated. At high alphas, the airflow on the rear wing is disrupted by the presence of the front wing. For the Gryphon, it was found that at an angle of attack of 10 degrees, this disruption occurs. This might present a problem to the performance of the aircraft.

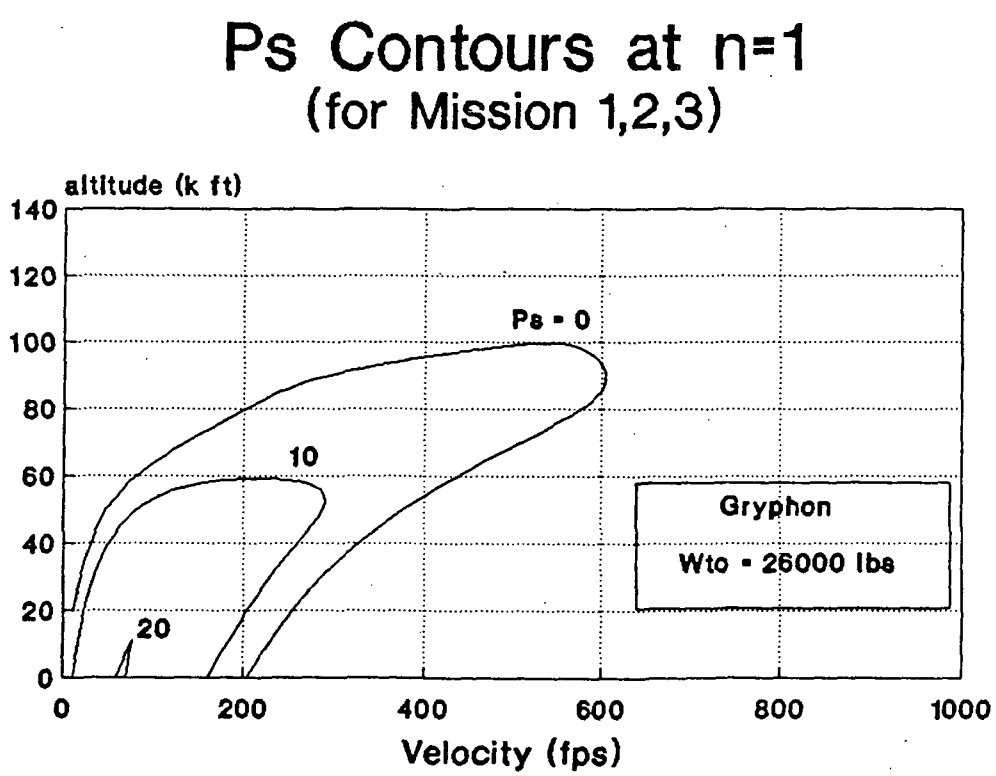

Figure 32

120,000 Feet: Mission #4

Figure 33 illustrates the absolute ceiling of the Mission 4 Gryphon aircraft at 110,000 ft. This does not meet the 120,000 feet excursion specified by the mission requirements. The power requirements needed to reach 120,000 feet were too demanding. A power available of 1600 hp (rated at 100,000 ft) would be needed. However, there are currently no engines available that can produce this much horsepower at that altitude.

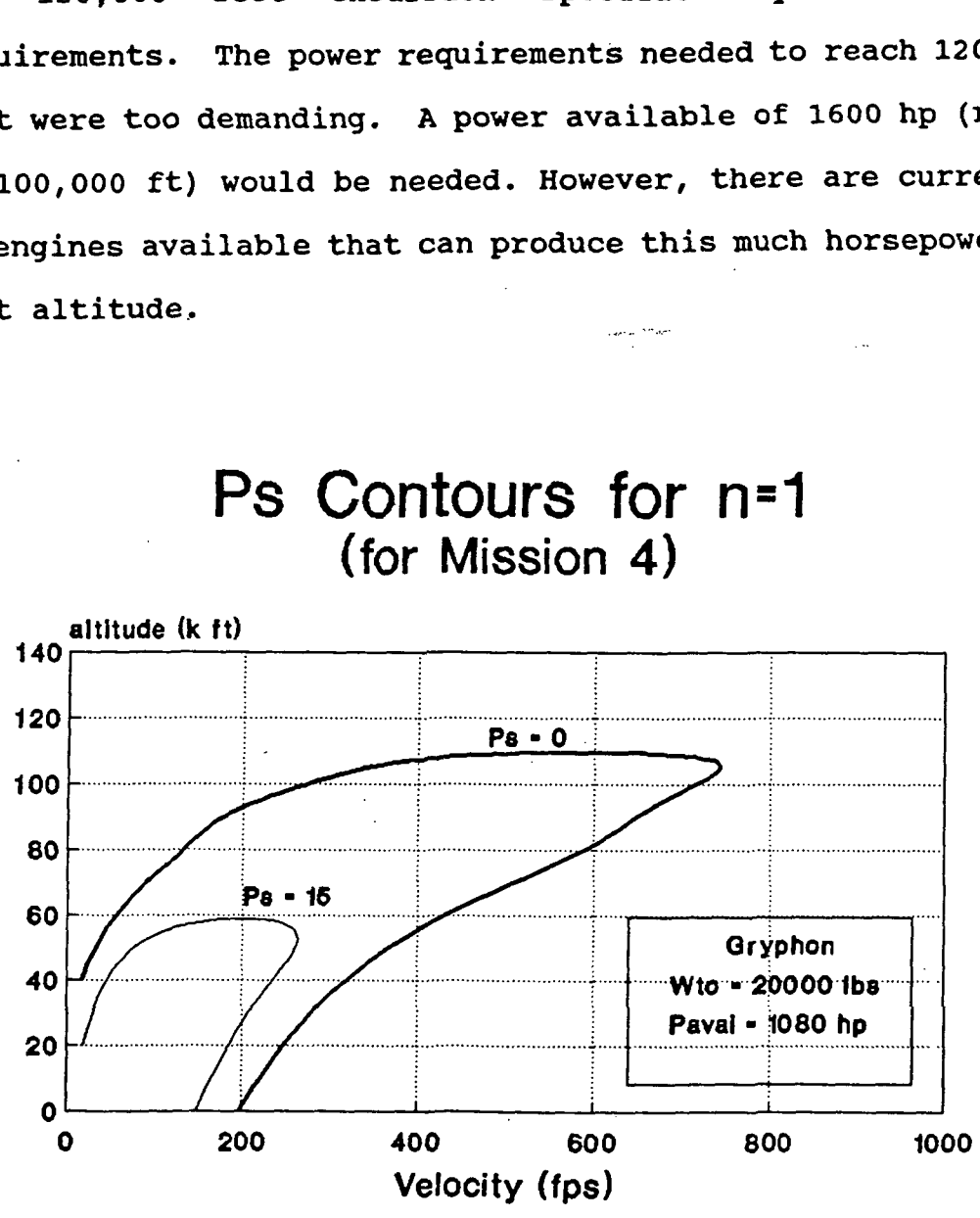

Figure 33

Using four GTSIOL 550's produces the necessary horsepower, but cooling these engines would produce an even more challenging problem. Increasing the wing aspect ratio will decrease the induced drag of the aircraft, thereby lowering the power requirements. However, the resulting decrease in the chord length might reduce the Reynolds number towards the laminar separation bubble regime. Higher aspect ratios are also limited structurally.

The technology needed to fly an aircraft to 120,000 feet is not currently available. Further research on engine cooling at high altitudes is recommended.

CENTER OF GRAVITY CALCULATION

The weights and locations of all major components were determined and used in the calculation for the center of gravity (c.g.) location of the aircraft. Figure 34 shows the location of the c.g. of the various major components. A spreadsheet program was developed to rapidly calculate and conveniently change the variables in determining the center of gravity location.

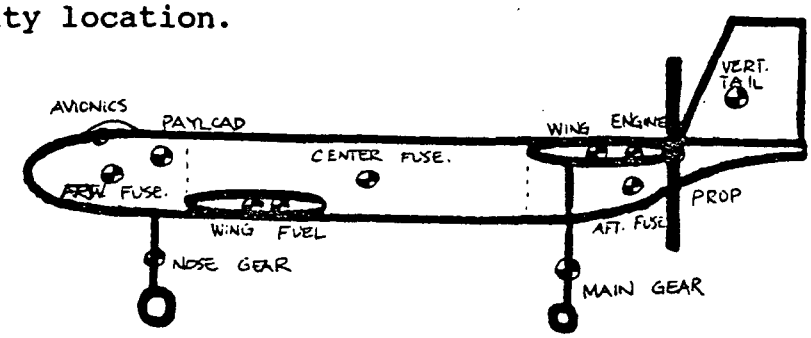

Figure 34: Center of Gravity for Major Components

Table 9 shows the calculation of the center of gravity at the flight condition of beginning cruise at 100,000 feet in the x-axis only, where the x-axis starts from the nose and goes toward the tail of the aircraft. The center of gravity was approximately 25.7 feet from the nose of the airplane for the calculation at gross take-off weight. The c.g. travels aft because the fuel is being burned off, thereby reducing the front wing's weight. At take-off, the c.g. is well forward of the aircraft's aerodynamic center (a.c.) at 25.3 feet. At the end of the cruise stage, the c.g. goes aft, behind the a.c. at 29.7 feet. The center of gravity

calculation affects the stability of the aircraft. Also, inertial calculations were estimated by using historical methods presented in Reference 15.

CENTER OF GRAVITY CALCULATION

COMPONENTS	WEIGHT (LB)	LENGTH X (FT)	MOMENT ARM (LB-FT)
WING (FRONT)	2594	17	44098
WING (REAR)	2551	42	107142
VERTICAL TAIL (L)	123	55	6765
VERTICAL TAIL (R)	123	55	6765
LEFT :			
FUSELAGE (NOSE)	180	6	1080
FUSELAGE (CENTER)	440	27	11880
FUSELAGE (AFT)	120	53	6360
RIGHT :			
FUSELAGE (NOSE)	180	6	1080
FUSELAGE (CENTER)	440	27	11880
FUSELAGE (AFT)	120	53	6360
ENGINE (L)	1700	43	73100
ENGINE (M)	1700	43	73100
ENGINE (R)	1700	43	73100
PROP (L)	100	48	4800
PROP (M)	100	48	4800
PROP (R)	100	48	4800
AVIONICS	400	7	2800
FRONT :			
MAIN GEAR (L)	180	16	2880
MAIN GEAR (R)	180	16	2880
REAR :			
MAIN GEAR (L)	220	44	9680
MAIN GEAR (R)	220	44	9680
FUEL (L)	3600	16	57600
FUEL (R)	3600	16	57600
FUEL (FUSELAGE)	200	31	6200
PAYLOAD	2500	8	20000
COCKPIT	250	7	1750
HYDRAULICS	100	35	3500
TOTAL	23721 LB.	854 FT.	611680 LB-FT.

C.G. (FROM NOSE) = 25.78643 FT (after climb, before cruise stag

Table 9: Center of Gravity Calculations

STABILITY AND CONTROL

Longitudinal Static Stability Analysis

With the configuration in Figure 2, the longitudinal static stability was calculated. An assumption made when using the program was that the longitudinal stability was not adversely affected by the twin fuselage configuration, only possibly the lateral stability. Therefore, the values of longitudinal stability derivatives obtained from the program were accurate. Table 10 shows the longitudinal stability derivatives.

Table 10: Longitudinal Stability Derivatives

Longitudinal Deriv.	Values (1/rad)	Criteria
Cm_{α}	-1.238	<> 0
Cm_{u}	0.000	< 0
Cm_{q}	-58.759	< 0
$Cm_{\delta e}$	-5.281	< 0
$Cm_{\alpha\text{-dot}}$	-11.790	< 0
CL_{α}	10.991	> 0
CL_{u}	1.594	0
CL_{q}	12.261	> 0
$CL_{\delta e}$	2.661	> 0
$CL_{\alpha\text{-dot}}$	5.941	> 0
CD_{α}	1.703	> 0
CD_{u}	0.000	<> 0
CL_{iH}	6.571	> 0
CM_{iH}	-13.041	< 0

Of these derivatives, the most important for meeting static stability is Cm_{α}. A negative Cm_{α} is desired for good longitudinal stability. The Gryphon has a Cm_{α} of -1.24/rad at flight conditions of 100,000 feet cruise. Figure 35 shows the range of c.g. affecting Cm_{α} for different flight

stages. Notice that the aircraft is stable at take-off, climb, and at the beginning of the cruise stage. As the fuel is used up during cruise, at 1/3 of the cruise stage, Cm_α becomes positive and the airplane is no longer statically stable. A solution for Cm_α being positive is to incorporate a pitch damper. This is discussed further in the design of stability augmentation for the aircraft.

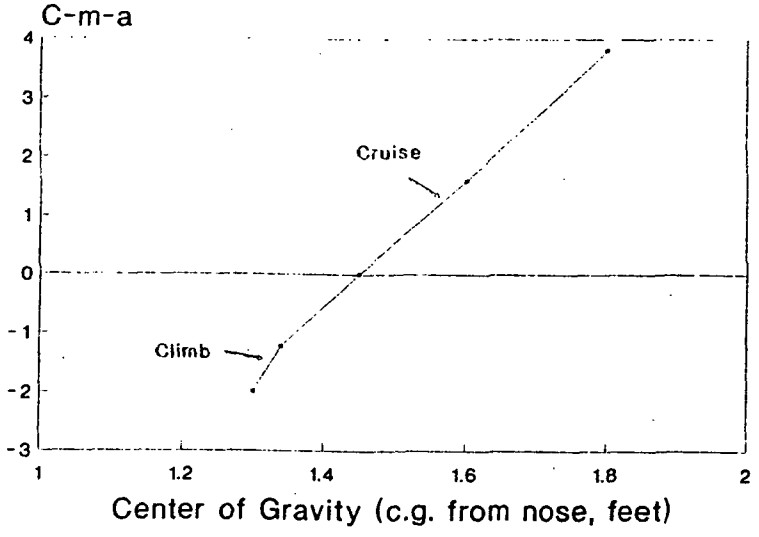

Figure 35: Effect of C.G. on Cm_α

Lateral Static Stability Analysis

Lateral stability derivatives were calculated using the same method in the determination of the longitudinal derivatives. Analysis of lateral stability was made more complicated by the twin fuselage configuration of the aircraft. Rather than alter the program, an assumption was

made to use one connected fuselage instead of the twin fuselage. Assuming this, the lateral stability derivatives calculated from the program will give us the general trend of what the stability derivatives are. From that, a stability augmenter, such as a Dutch roll damper, can be implemented to help stabilize the aircraft in the lateral direction. Table 11 lists the lateral stability derivatives.

Table 11: Lateral Stability Derivatives

Lateral Deriv	Values (1/rad)	Criteria
Cn_b	0.023	> 0
Cn_p	-0.504	<> 0
Cn_r	-0.206	< 0
$Cn_{\delta R}$	-0.085	< 0
$Cn_{\alpha R}$	-0.004	< 0
Cl_b	-0.244	> 0
Cl_p	-0.946	< 0
Cl_r	0.944	> 0
$Cl_{\delta A}$	0.336	> 0
$Cl_{\delta R}$	0.002	> 0
Cy_b	-0.612	< 0
Cy_p	-0.343	< 0
Cy_r	0.053	> 0
$Cy_{\delta A}$	0.000	0
$Cy_{\delta R}$	0.086	> 0

Notice the important derivatives are those of the rolling moment coefficient due to the sideslip angle (Cl_β) and of the yawing moment coefficient due to sideslip angle (Cn_β). A negative Cl_β is desired and achieved in the aircraft, but it is small.

Controllability

Dynamic Stability Analysis

A dynamic analysis of the Gryphon was performed using AFDA, a flight dynamics program, for the cruise flight conditions of M = 0.6 at 100,000 feet, with a full payload. Using the stability derivatives calculated in the previous section, the roots of the characteristic equations were found. Table 12 lists the roots of the characteristic equation. Note that the roots are either negative real roots or complex conjugates with negative real parts indicating the stability of the aircraft.

Table 12: Roots of the Characteristic Equation

Longitudinal	Lateral
S1 = -0.004 + j 0.086	S1 = -0.011
S2 = -0.004 - j 0.086	S2 = -1.367
S3 = -0.503 + j 1.238	S3 = -0.746 + j 1.769
S4 = -0.503 - j 1.238	S4 = -0.746 - j 1.769

Next, the longitudinal and lateral direction modes were determined. The longitudinal short period and phugoid modes, and the lateral Dutch roll, spiral, and rolling modes are listed in Table 13.

Table 13: Longitudinal and Lateral Direction Modes

Direction Modes	Frequency (rad/sec)	Damping Ratio
Short Period	1.465	0.376
Phugoid	0.086	0.065
Dutch Roll	1.921	0.388
	Time Constant	
Spiral	84.601	
Rolling	0.259	

The short period has adequate damping of 0.68, but the phugoid mode has low damping. For lateral modes, the Dutch roll has adequate damping also.

Time responses were created for the longitudinal and lateral cases. The longitudinal perturbations were caused by a step elevator deflection of 10 degrees, while the lateral perturbations were caused by step rudder deflections of 10 degrees. It was noticed that the longitudinal time responses were all oscillatory, but damped. The lateral time responses indicated the roll and sideslip were damped. However, the yaw perturbation was divergent. A stability augmentation system was designed to correct this problem.

Autopilot and Stability Augmentation

In designing the autopilot for the Gryphon, the method presented in Reference 2. A pitch displacement autopilot and a pitch displacement autopilot with rate feedback were compared. Using a simulation software package called Program CC, the root loci of the displacement autopilot and the autopilot with rate feedback were created and are shown in Figures 36 and 37.

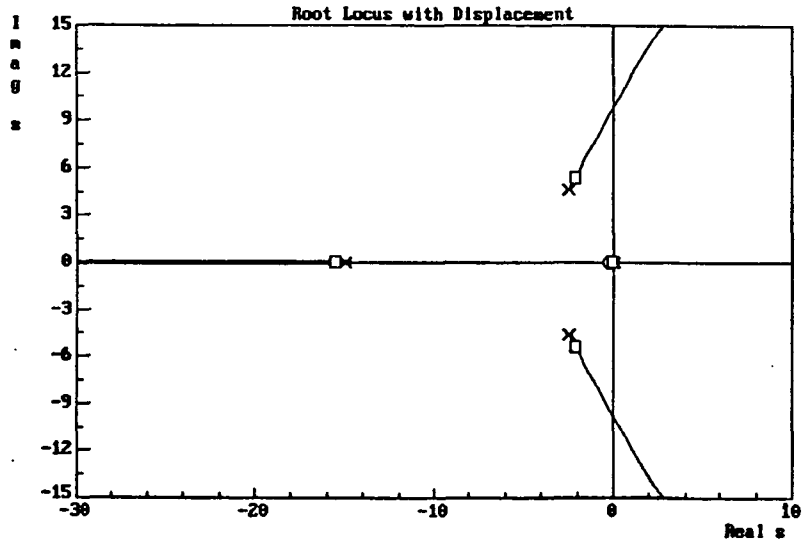

Figure 36: Root Locus with Displacement Autopilot

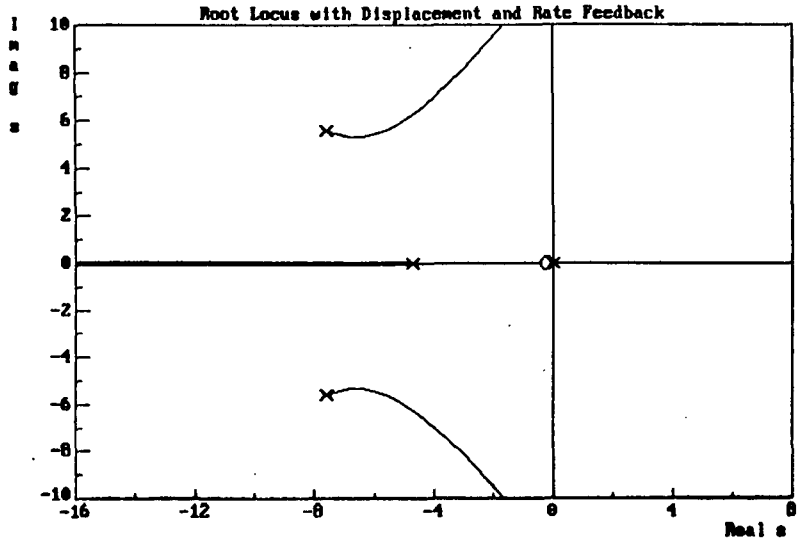

Figure 37: Root Locus with Displacement and Rate Feedback

The displacement autopilot with rate feedback shows a definite larger damping than without rate feedback. Therefore, the displacement with rate feedback provides better damping in the longitudinal direction. The block diagram for the displacement autopilot with rate feedback is

shown in Figure 38. The time response is plotted in Figure 39 and shows a smooth, damped response for the autopilot.

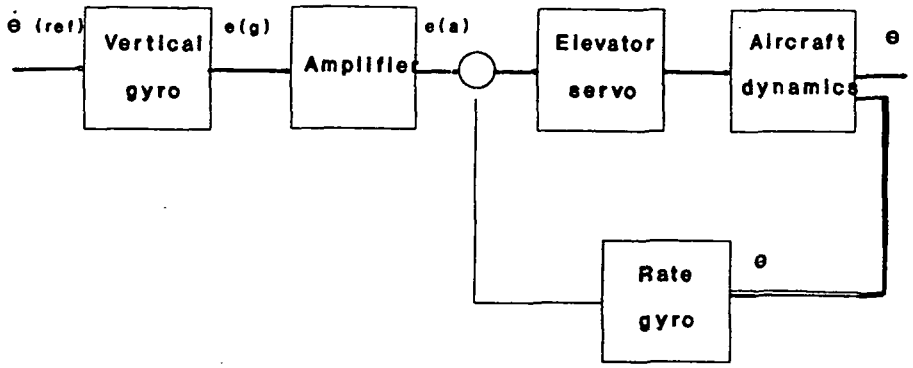

Figure 38: Displacement Autopilot with Rate Feedback

Figure 39: Time Response with Displacement and Rate Feedback

The Yaw Orientational autopilot was used for the lateral direction. This system consisted of a Dutch roll damper combined with sideslip for coordination, and a roll rate feedback loop. The inputs are the commanded yaw rate, which produces a turn, and the pilot's rudder input. This

autopilot is capable also of accepting commanded heading changes. The block diagram for the yaw orientational autopilot is shown in Figure 40.

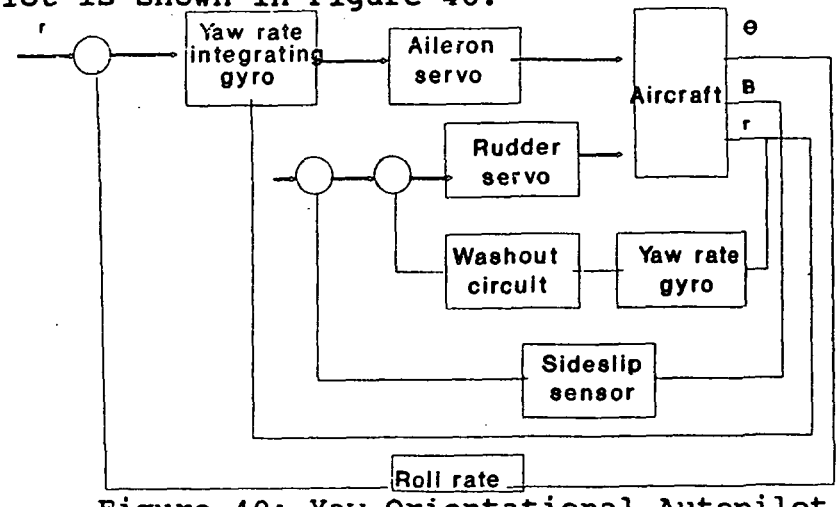

Figure 40: Yaw Orientational Autopilot

The Dutch roll damper is used to damp the Dutch roll mode. Figure 41 shows the root locus of the damped aircraft. Notice that it is slightly damped. Since maneuvers are often performed with a resulting lack of coordination, a coordination technique was incorporated. Figure 42 shows the root locus with sideslip coordination.

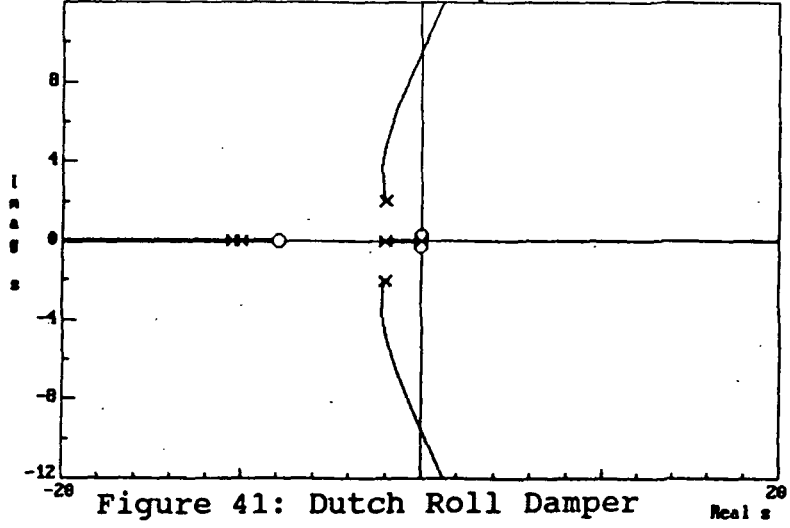

Figure 41: Dutch Roll Damper

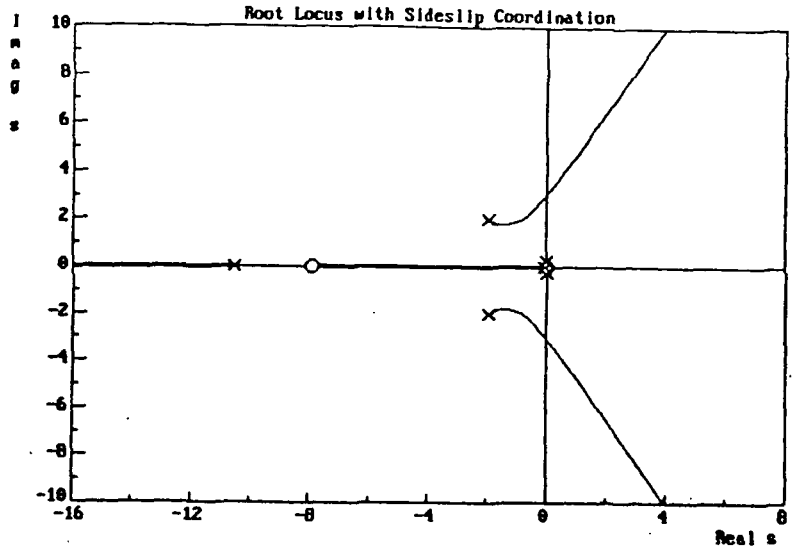

Figure 42: Root Locus with Sideslip Coordination

With the Dutch roll damper and the sideslip coordination, the yaw orientational autopilot was designed. The root locus of Figure 43 shows that the airplane is adequately damped. Overall, the autopilots that were created managed to stabilize the Gryphon and provide better responses. This can be seen easily in Table 14.

Table 14: Comparison of the Effect of Adding Autopilot

Mode	Gryphon	w/Autopilot
Short Period		
Damping Ratio	10.376	0.701
(rad/sec)	1.465	7.913
Dutch Roll		
Damping Ratio	0.388	0.710
(rad/sec)	1.921	2.644

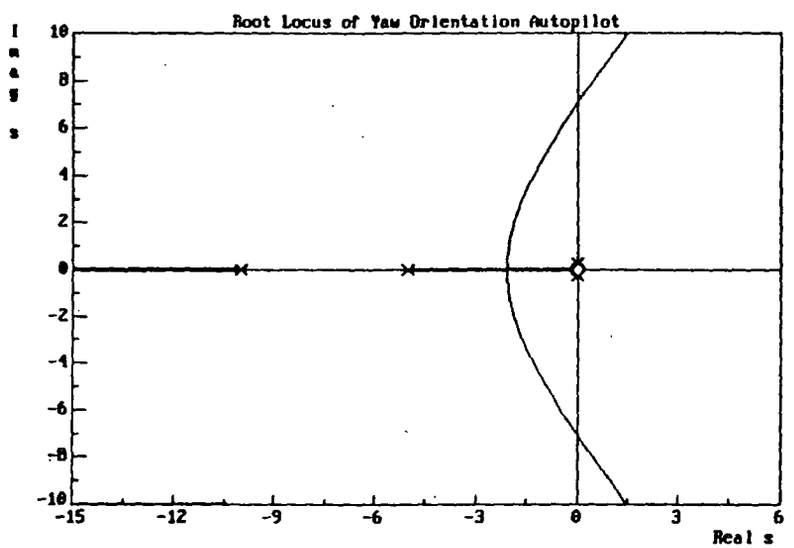
Root Locus of Yaw Orientation Autopilot
Imag s
10
8
6
4
2
0
-2
-4
-6
-8
-10
-15
-12
-9
-6
-3
0
3
6
Real s

Figure 43

Flying Qualities

It is important to the pilot that certain modes of motion of the aircraft are well behaved. Mil-F-8785B shows some insight in what constitutes good handling quality characteristics in terms of mode and mode shape characteristics. Even though the Gryphon is not strictly in the military plane classification, Mil-F-8785B is used for the lack of other references in comparing flying qualities. Definition of the airplane class for the Gryphon is Class II, which constitutes aircraft with medium weight, with low-to-medium maneuverability. Such aircraft in this class include light transport and reconnaissance aircraft. Also, the flying quality level is Level 1 and Category B for cruise.

The requirements for minimum phugoid and short period damping are shown in Table 15. The requirements for spiral stability, Dutch roll stability, and roll mode stability are also shown in this table.

Table 15: Flying Qualities Requirements (Mil-F-8785B)

Mode	Gryphon	Mil-F-8785B	
	Damping Ratio	Min	Max
Short Period	0.681	0.30	2.00
Phugoid	0.065	0.04	----
Dutch Roll	0.663	0.08	0.40
	Time Constant	Min	Max
Spiral	89.766	20.0	----
Roll Mode	0.730	----	1.40

Control Surfaces

Trim and pitch control is provided by flaps located on the inboard sections of the front wing. Yaw control is provided by the rudders on the twin vertical tails. The rudders were sized to maintain control during one engine-out situations. The rudders are also capable of controlling the aircraft with 15 knot crosswinds and moderate turbulence conditions. Roll control is provided by ailerons located on the four outboard sections of the tandem-wings. To maintain the same relative lift between the tandem-wings at all times, all four ailerons will have to be deflected simultaneously. Because of the unusual configuration of the Gryphon, controlling the aircraft might become unpredictable. A fly-by-wire flight control system is recommended.

HUMAN FACTORS

Manned vs. Unmanned Study

The high altitude research aircraft needs to reach an altitude of 100,000 ft. At this altitude there is a need for 100% use of a liquid oxygen converter for the case of man-in-cockpit. This also requires redundant life support systems, such as the full pressure suit, suit-cooling air source, suit faceplate heat, and air-conditioning. A system for the pilot to pass urine from the suit to a cockpit reservoir is required, as well as a place for food storage.

In the case of a manned mission, the pilot can monitor the output of payload data and change the course of the Gryphon if it seems viable for data collection. However, the longest mission time is approximated to be at most 16 hours long and the shortest mission time is about 10 hours long. The pilot is constrained to both a pressure suit and lack of mobility within the narrow cockpit. At present the Gryphon may not be capable of supporting the additional weight of a pilot and required life support systems.

The recommendation is for an unmanned aircraft. The aircraft can reach 100,000 ft, but currently is not capable of carrying the extra payload weight to sufficiently provide 100% safe and efficient life support. The control of this unmanned craft will be discussed later.

Avionics

The general control system of the Gryphon consists of indicators and controls for flight, fuel, engine, and payload. The Gryphon will receive commands from the remote pilot, and will carry a high performance INS/GPS Integrated Navigation System on board to provide navigation data of an accuracy and consistency not available from a single navigation system throughout long duration flights. Without too much trouble, the Gryphon can be converted to the on-board pilot configuration in case it is necessary to carry out manned missions or to practice presentation flights or ferry flights which would be too taxing for the remote-control gear.

High Performance INS/GPS Integrated Navigation System

The Integrated Navigation System to be described is required to provide the following functions throughout long duration flights:

a) Navigation data of an accuracy and consistency not available from a single navigation system.

b) Effective navigation on the failure of any single navigation sensor or during the loss of GPS data due to maneuvering, jamming or GPS control of space segment failure.

c) High accuracy autonomous Inertial Navigation System performance when no other sensors are available.

d) Warning that any sensor is failing or has failed, from the detection of degraded sensor performance to a gross sensor failure.

e) Comprehensive validity checks on all the sensor data. This includes comparison of the INS data with GPS and the comparison of the pseudo-ranges and range rated between the satellites being tracked.

f) In-flight calibration of the sensors to eliminate the need for routine ground calibration.

The system incorporates a 4-gimbal inertial navigator of inherently high stand-alone performance, integrated with a state-of-the-art 5 channel P-code GPS receiver. The system partitioning and interfacing are configured to optimize system accuracy during potentially lengthy periods when a full GPS solution may be unavailable, while providing satisfactory integrity under reversionary conditions.

The primary sensors for INS are an Inertial Navigation system, a GPS receiver and antenna system and an Air Data Computer. Secondary sensors which may be used under reversionary conditions are Omega, Radar Altimeter and Gyro Magnetic Compass. Using these sensors, the INS provides the best possible position, velocity, attitude and heading information to the rest of the aircraft systems.

The receiver should be capable of using rate-aiding data to compensate for antenna motion and should have a 5

channel P-code receiver to prevent loss of lock to improve its jamming resistance.

Inertial Navigation System Performance

The Integrated system provides very high accuracy position and velocity data at all times. When GPS is available, the integrated system outputs have the long term accuracy of the GPS with the superior short term characteristics of the INS. The accuracy is largely independent of the quality of the INS. However, when GPS data is unavailable due to either jamming, non-availability of satellites or a failure of some part of the GPS sub-system, the Kalman filter can only propagate the state estimates existing prior to the loss of the GPS data. The inertial system error sources must therefore be stable in-run to ensure that these estimates remain valid when no update measurements are available.

The most extreme case occurs when no GPS data is available at any time during the flight, in which case the Integrated Navigation System performance will be that of the Inertial Navigation System. In order to meet the stand-alone accuracy requirement for the INS, the error sources must be stable from run-to-run so that calibrations obtained from a previous flight when GPS was available may be used. If they are not sufficiently stable then some pre-flight calibration procedure must be carried out in order for the

INS to meet the autonomous accuracy requirement. The particular error sources and their stability and effect on INS performance are discussed later.

The Inertial Navigation System must be capable of highly accurate stand-alone performance and must therefore have stable instrument error sources. The type of currently available INS that best meets these requirements for high position and velocity accuracy is a gimbaled system using conventional floated rate integrating gyros or dry tuned gyros.

Remote Pilot

Remote control is exercised from two remote stations, one fixed, the other mobile. On board the Gryphon are three basic installations which make remote control possible: the autopilot, a command/telemetry data link, and an interface coupler for processing the data which passes to and from the RPV from the remote control positions, within the automated control system is the stability augmentation system and the structural integrity assessment system.

Control System

The control system for the control and trim surfaces (the ailerons, rudder, and stabilizers) consists of fly-by-wire communications controlling hydraulic actuators. The electronic and hydraulic buses are both star-type configurations, thus all communication signals and pressure

lines originate from a central location, which makes each subsystem independent and safer. Each actuator has its own pump, step servomotor, and separate hydraulic system. All the subsystems are linked together into a main hydraulic system which has a reservoir and pressurization pump.

Cockpit

The cockpit features module instrumentation panels for life support systems to sustain a pilot to be installed for a manned flight as an option. The dimensions of the cockpit are: width - 3 ft, height - 7 ft, depth - 16 ft.

For comfort, all the control panels are laid out such that the pilot can reach them without any undue effort and also allows room for the pilot's seat and his pressure suit. (See Figure 44.) The pilot must wear a pressure suit which is attached to portable environmental units.

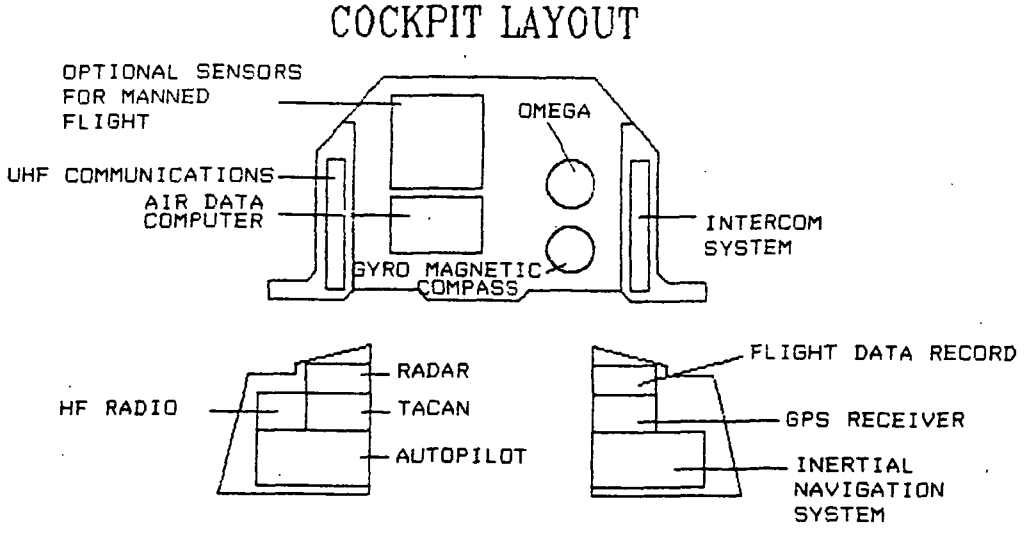

Figure 44

Avionic Equipment (Unmanned)	Weight (lbs)
Inertial Navigation System	207
GPS Receiver	10
TACAN	61
Air Data Computer	14
Omega	10
Radar Altimeter	38.2
Gyro Magnetic Compass	8.4
Autopilot System	168.5
Intercom System	19.2
UHF Communication	11
HF Radio	78.4
Flight Data Recorder	15.6

Total Avionics Weight	641.3

SURVIVABILITY

Since this aircraft does not operate in a highly volatile environment, there are no ejection seats. In the event of a power failure or internal fuselage fire, the Gryphon is capable of gliding to a safe landing site. If the fire in any way endangers the pilot's life, the pilot has the option of parachuting out of the Gryphon after it has glided down to an altitude deemed safe and survivable for the pilot. However, this leaves the Gryphon under the control of the autopilot which should be able to reach the designated landing site in the case of an internal fuselage fire.

The following is a chart that shows some key preliminary issues:

Survivability Issues

- Hierarchy of Survivability
  1. Mission Continuation
  2. Optimum Return to Base
  3. Landing
  4. Trim to Fly
  5. Engine Out Glide

Mission continuance means that the plane has as much of the primary flight control capability available as originally on the aircraft. The next notion is that an optimal return to base. Landing requires some Level III

flying qualities under "nice conditions". If there are gusty conditions, the plane may not make it. The Gryphon is capable of meeting the issues of survivability, whether manned or unmanned. The payload should be able to survive intact even if the Gryphon crashes.

It should be noted that in case of a crash landing, the fuel that is stored in the lower front wing could ignite. The high lifting capabilities of the Gryphon should be able to prevent a belly landing on this wing. The propellers would break away, and the rear area of the fuselages would be destroyed, but the fuel tanks should be safe.

Ground Service Features

Fuel, hydraulic and GN2 carts will be necessary to service the aircraft. The fuel cart will provide refueling and defueling functions. The hydraulic cart will provide hydraulic fluid with purge and fill functions. The ground nitrogen carts pressurize or depressurize GN2.

MANUFACTURING

Pre-fabricated subassemblies will be attached to the aircraft superstructure in stages. The first stage consists the skeleton of the wing, the major component of the airplane. The load carrying beam is braced and the ribs are affixed in their designated locations. Next hydraulic control systems, fuel pumps, and bladder type fuel tanks will be installed, including any special sensors or electrical controls key to the design of the Gryphon. The fuselage (stringers and skin) and cockpit will be laid out next in accordance with the wing structure. Any special cooling flow lines will be installed at this point between the fuselage and the wing. The electrical wiring and hydraulic lines will be placed in the routing tunnel in the upper oval of the elliptical fuselage. The cooling skin on the wings will be manufactured separately and will be fastened to the superstructure of the Gryphon at the same time as the leading edge buildup and control surfaces. Cargo compartments, pilot support equipment, and landing gear will integrated after initial assembly is complete.

It is expected that the flat-wrap curvature used in the elliptical construction of the fuselage will result in significant cost savings. The tail cone presents no problem because it can be linearly scaled to produce a flat-wrap surface. These design considerations will greatly reduce

the tooling costs and fabrication manhours, which plagues designs that employ any type of three dimensional curvature.

Production breaks divide the subassemblies at the cockpit, the aft fuselage, and five mid-fuselage subassemblies. The front landing gear will be placed immediately in front of the cockpit-fuselage production break to avoid crossing the break line which sometimes leads to unmatched dimensioning between the two sections. Quadricycle landing gear will facilitate production cost reduction due to the commonality in parts for the left and right landing gear components. The breakdown of the manufacturing of the Gryphon can be seen in Figure 45.

MANUFACTURING AND ASSEMBLY OUTLINE

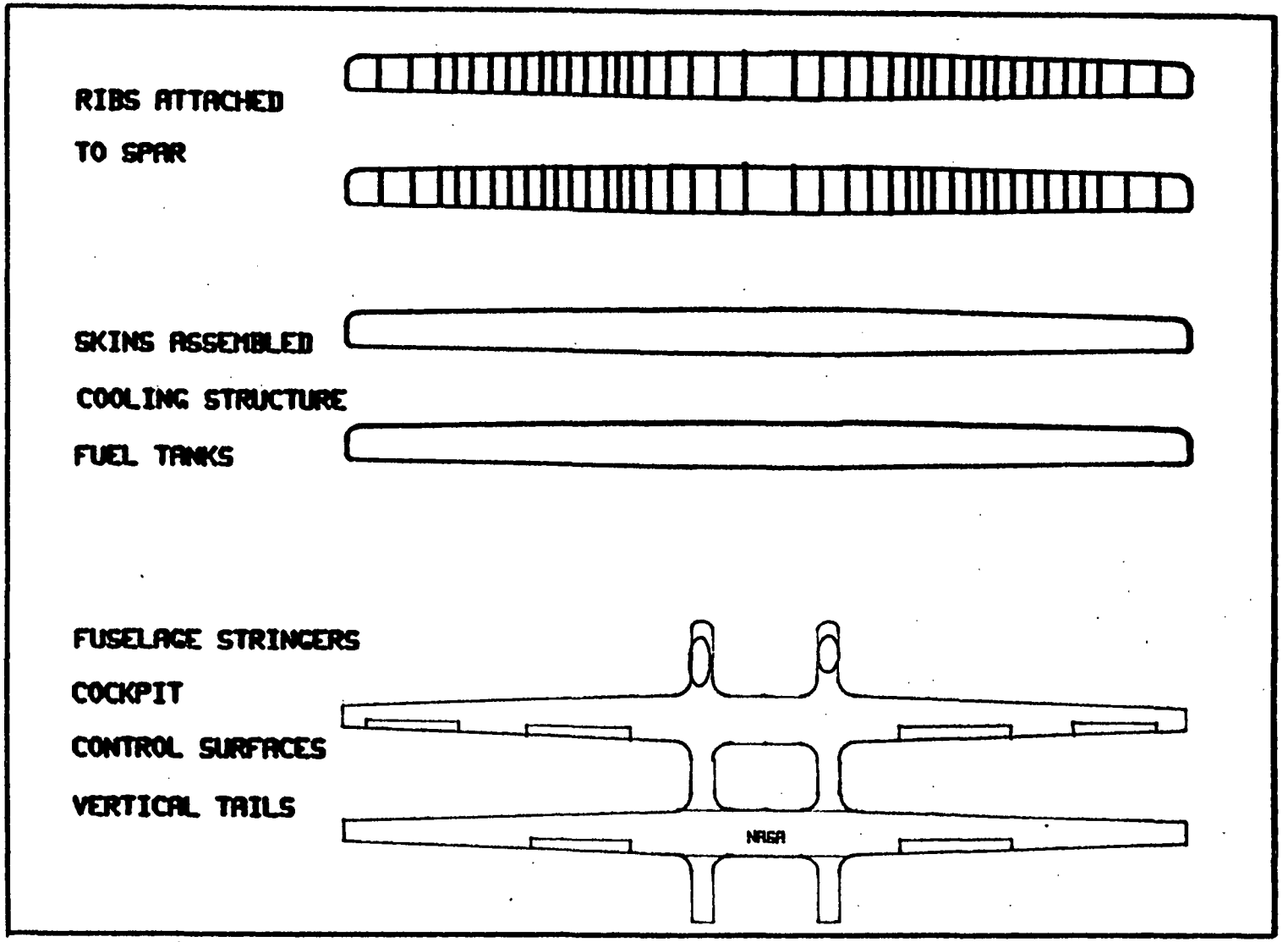

Figure 45

Quality Control

The question of whether or not to install quality control is influenced by the following factors. Is the product a high precision product? Is quality checking a lengthy process? Is defective work a common reality? Since the answer to all of these questions is "yes" when considering the producibility of the Gryphon, the installation of quality control is deemed necessary in its production process.

Several types of quality control exist including screening, lot-by-lot inspection, process inspection, reliability testing, and the systems approach. Since screening 100% of the individual pieces is not a cost effective approach when dealing with such a specialized aircraft, process inspection used in conjunction with reliability testing offers the most practical approach. When installing quality control several aspects of this approach must be taken into consideration including: Control Charts, Control of Variability, Process Capability, Product Tolerances, Vendor-Vendee relations, and Organization. In order that all of these aspects be taken into account a Total Quality Control Chart is drawn in Figure 46. Through this chart we can visualize how the quality of raw stock, and the reliability of processes influence the entire manufacturing process. Planned and goal conscious word is

essential in the installation, maintenance, and growth of economical and effective quality control and product reliability. It is through this plan that customer satisfaction and the product's name are built.

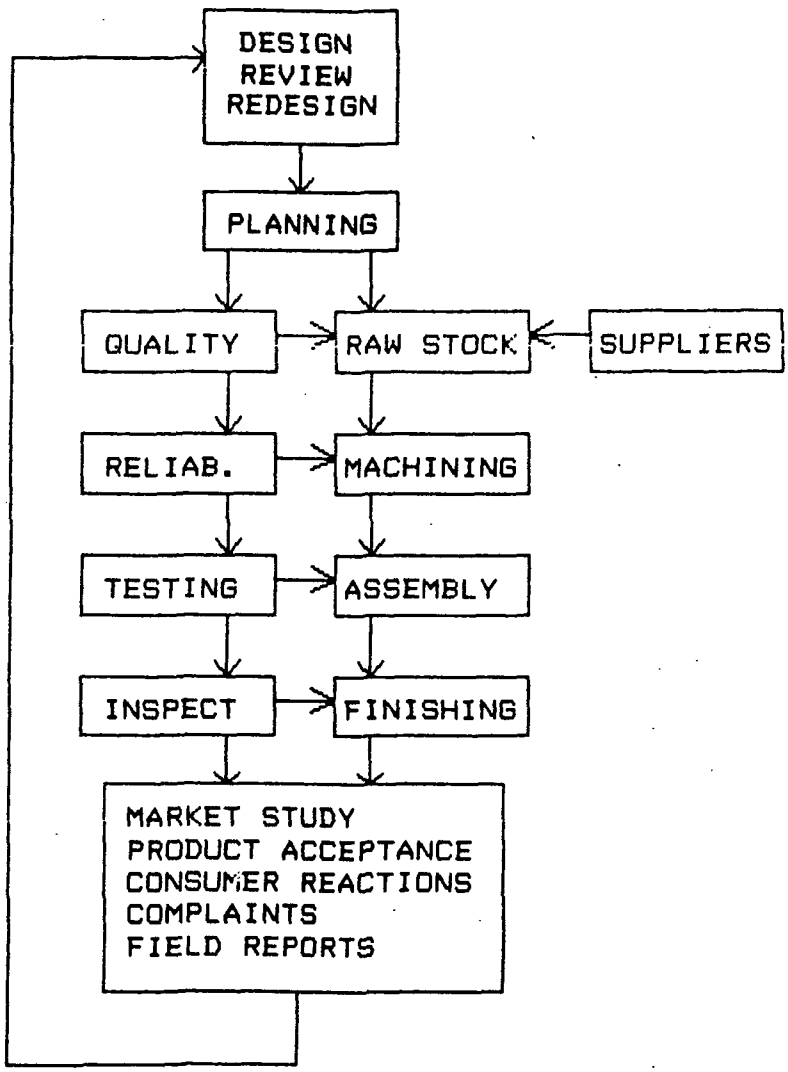

Figure 46: Total Quality Control Chart

Management

In developing complex products it has become customary to establish a "program" or "project" type of organization. In the pure project type of organization, a program manager is appointed by top management and is given the responsibility and line authority for all program objectives, cost schedules, and technical performance. In this way responsibility will be centralized which will help provide for rapid development of the new system and for good communication between contractor and customer. Figure 47 illustrates the management plan.

Potential compromises of performance objectives resulting from program managers' decisions are subject to the check and balance provided by routine contact with the functional organizations from which program personnel were borrowed. Conflicts do arise, but when all concerned have experience with this form of organization, the conflicts are viewed as a normal mode of operation that helps to provide balance among cost, schedule, and performance. A generalized organization chart can be useful in outlining the relationship between the audit aspects of management with the traditional functions.

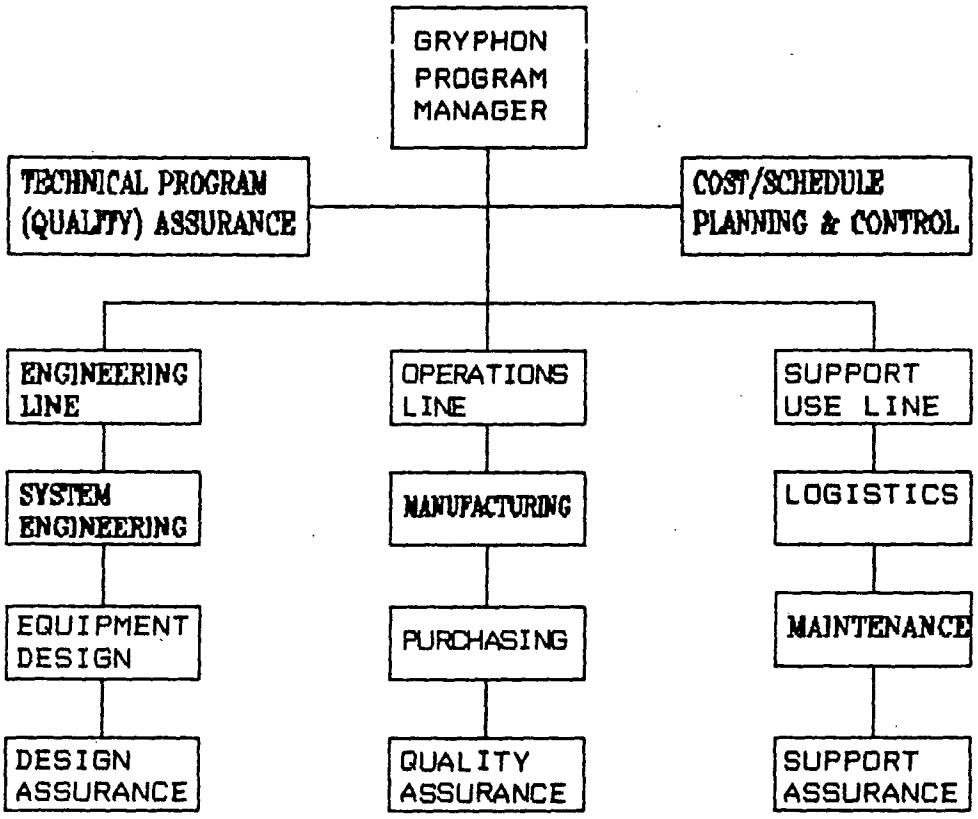

Figure 47: Management Plan

Maintainability

Maintainability simply means the ease with which the aircraft can be fixed. Reliability and maintainability are frequently bundled together and measured in Maintenance Manhours Per Flighthour (MMH/FH). MMH/FH is roughly proportional to weight because the parts count and system complexity go up with weight. Reliability is usually out of the hands of the conceptual designer. It depends largely upon the detail design of the avionics, engines, and other subsystems. The only way for the configuration to negatively impact reliability is by placing delicate components, such as avionics, too close to vibration and heat sources, such as engines. For the Gryphon aircraft, the avionics are placed in the front fuselage where vibration is minimal since it is not near the fluctuating wings. Also, the Gryphon's avionics are away from the heat source of the engines. The engines are attached to the back wing along the span.

The major driver for maintainability is the accessibility. Accessibility depends upon the packaging density, number and location of doors, and number of components that must be removed to reach the broken component. As a general rule, the best access should be provided to the components that break most often or require the most routine maintenance.

Engines are a good example of these types of components. The engines are located in the lower half of the rear wing, with the engine access door able to open downwards in order to facilitate maintenance, repairing, or possible removal of the engine from the aircraft nacelle. These types of access doors are also provided for the avionics compartment, hydraulic pumps, actuators, environmental control systems, and the auxiliary power unit. The worst feature that an airplane can have for maintainability is a requirement for structural disassembly. The Gryphon does not have any structural components that require disassembly for component removal.

Design Scheduling

The basic design of the Gryphon has already taken 9 months to accomplish. Much more research is needed in areas such as cooling, attaining the 120,000 foot altitude goal, and analyzing all of the stresses and strains that will be placed on the wing and fuselage structures. This research should be conducted and completed by 1992. At this point, feasibility studies should be performed on the materials manufacturing to check the cost of materials and tooling for the craft. A detailed manufacturing plan will have to be created, so that manufacturing engineers will be able to set up a factory for production.

By the year 1993, this plan should be created. The quality control groups should have monitored the plan so that any product testing that will be required will be possible. 1994 through 1996 will be the years during which the Gryphons will be produced. By 1997, the aircraft should be ready for flight testing, beginning with lower altitude endurance flights, and leading up to high-altitude excursions. 1998 will be the year during which the Gryphon will prove its performance capabilities, as the flight tests broaden their range and demands. Finally, the aircraft will be ready for use in 1998.

The four missions that need to be flown can be done repeatedly, or as needed for data collection regarding the

ozone layer deterioration. Due to its high-altitude and long range capabilities as either a manned or unmanned airplane, the Gryphon will not be limited in its applications. The Gryphon could be used for other flights, such as to gather information about other global regions while remaining above radar levels, for testing that is currently utilizing sounding rockets and balloons, and for a variety of missions.

The estimated lifespan of these airplanes is 20 years. This is due to the fact that after the information has been gathered on the ozone depletion, possibly within three years of the first mission, the Gryphon will no longer be required for these types of flights. Rather than "retiring" the aircraft, it will remain a useful plane, flying occasional missions until it is worn down of obsolete. Even with maintenance, the plane is not expected to be useful past 2020.

COST ESTIMATION

For the Production of 2 Planes

Materials & Parts	**Estimate**
Avionics/Flight Control	450,000
Electrical & Lighting	30,000
Fuel	20,000
Hydraulics	225,000
Propulsion	525,000
Airframe	350,000
Total Material Cost	**1,600,000**
Labor Costs	
Engineering/Development	990,000
Tooling	390,000
Quality Control	110,000
Manufacturing/Production	670,000
Test Flight	140,000
Total Labor Costs	**2,300,000**
Total Cost for 2 Gryphons	**3,900,000**

Comparison to Similar Aircraft

B1-B Bomber	$150,000,000
TR-1	$ 14,600,000

This cost estimate was prepared by breaking down the total cost of an airplane into 2 broad categories: Materials and Parts, and Labor Costs. The estimates were found based on published data from other aircraft during recent years. In comparison to similar airplanes, such as the B1-B Bomber and TR-1, the Gryphon costs much less to manufacture and produce. The total cost for 2 airplanes designed as the Gryphon would be is 3.9 million dollars.

Table 16: RFP Requirements

Topic	RFP Requirements	Gryphon
Mission Profiles	1, 2, 3, and 4	1, 2, 3
Manned/Unmanned		Unmanned
Runway	Distances/Clearance	Meets
Crosswind Capability	15 knots	Meets
Low W/S Landing		Aileron & Elevator Combo
Safety & Flexibility	2 engines	3 engines
Hangar	110' x 70'	Proposed

The RFP was very specific about some of the requirements that the airplane design must feature, such as the minimum number of engines. These requirements were met by the Gryphon design. The only two portions of the RFP that were not met were the excursion to 120,000 feet in Mission four and the ability to fit the aircraft into the designated hangar. The engine that is being used for the this design is the GTSIOL 550 with three stages of turbocharging. This engine is still in the production stage, with testing ongoing. It was originally thought that this engine would be able to provide 500 horsepower at 100,000 feet, but it was found that it derates 20% at that altitude. It is possible that an engine will be designed in the future to provide more power at altitude, so that the Gryphon can meet the altitude requirement.

The Gryphon has a wingspan of 202 feet. It is obvious that the plane will not fit into the hangar that is only 110

feet long. A tradeoff study was performed in order to find the best way to accommodate the airplane. If the wings of the craft were removed after flight, the plane would fit into the hangar. However, the operating and maintenance costs increase when this extra work needs to be done because machinery, such as a forklift would be required, as well as the people to operate the machines. The reliability of the airplane decreases because the wings are no longer made of one solid structure with complete spars running through them. Also, the area where the detachment would take place would have to be reinforced, thereby increasing the weight of the Gryphon. The drag of the plane will increase because of the additional attachments and weight, causing the design to suffer tremendously.

It was discovered that it would be a better investment to build a new hangar with increased dimensions for the Gryphon. Although the initial cost would be high, the overall results would prove to be more favorable, especially in the performance and overall cost of the Gryphon.

CONCLUSION

After nine months of extensive research and analysis of the Gryphon, a tandem - wing twin - fuselage aircraft, it has been determined that this aircraft is suitable for the high-altitude missions that are specified in the RFP. The major design drivers have been thoroughly addressed, and almost all of the problem areas have been resolved. The data contained within this report and all of the calculations that were performed to achieve this data, prove that the Gryphon is an airplane design that will not fail!!

REFERENCES

1. Anderson, John
   Introduction to Flight.
   McGraw-Hill Book Co.
   NY, 1985

2. Blakelock, John
   Automatic Control of Aircraft and Missiles.
   John Wiley and Sons Inc.
   NY, 1965

3. Curry, Norman
   Landing Gear Design handbook, First Edition.
   Lockheed Georgia Co.
   Ga, 1982

4. Ebeling, Alvin
   Fundamentals of Aircraft Environment.
   Hayden Book Co.
   NY, 1978

5. Dodbele, S.S.
   "Shaping of Airplane Fuselages for Minimum Drag"
   AIAA-86-0316, Jan. 1986

6. Hagen, Roy
   Advanced Turboprop Project.
   NASA Scientific and Technical Information Division
   Washington, D.C., 1988

7. Hoak, D.E.
   USAF Stability and Control Datcom, Flight Control
   Division, Air Force Flight Dynamics Laboratory
   Wright Patterson Air Force Base, Ohio

8. Khan, F.A.
   "Tip/Vortex/Airfoil Interaction for a Canard/Wing
   Configuration at Low Reynolds Numbers"
   AIAA-89-0536, Jan. 1989

9. Liebeck, R.H.
   "Vortex Generators Used to Control Laminar Separation
   Bubbles"
   AIAA-90-0051, Jan. 1990

10. Lissaman, P.B.S.
    "Low Reynolds Number Airfoils"
    Annual Review of Flight Mechanics, Vol. 15, 1983

11. Maughmer, M.D.
"An Airfoil Designed for a High-Altitude Long-Endurance Remotely Piloted Vehicle"
AIAA-87-2554, Aug. 1987

12. McCormick, Barnes
Aerodynamics, Aeronautics, and Flight Mechanics.
John Wiley and Sons
NY 1979

13. Raymer, Daniel
Aircraft Design: A Conceptual Approach.
American Institute of Aeronautics and Astronautics
Washington, D.C. 1989

14. Reuther, J.
Subsonic and Transonic Low Reynolds Number Airfoils with Reduced Pitching Moments.
AIAA-90-3212, Sept. 17-19

15. Roskam, Jan
Airplane Flight Dynamics and Automatic Flight Controls Part 1.
Roskam Aviation and Engineering Corp.
Kansas 1979

16. Agard.
NATO Agard Lecture Series #166

17. NASA Reference Publication 1162
Present State of Knowledge of the Upper Atmosphere.
May 1986

18. NASA Conference Publication 2279
Controls, Display, and Information Transfer.
Oct. 1983

19. MIL-F-8785C
Military Specifications
Flying Qualities of Piloted Airplanes

All information regarding the Teledyne Continental GTSIOL 550 engines was provided by Teledyne Corporation.